ResearchGate

See discussions, stats, and author profiles for this publication at: https://www.researchgate.net/publication/260330606

Carbon Materials for Fuel Cells

Chapter · January 2014

DOI: 10.1007/978-94-007-7708-8_7

CITATIONS
3

READS
1,848

2 authors:

Mariano Bruno
National Scientific and Technical Research Council
35 PUBLICATIONS **495** CITATIONS
SEE PROFILE

Federico A. Viva
Comisión Nacional de Energía Atómica
34 PUBLICATIONS **515** CITATIONS
SEE PROFILE

Some of the authors of this publication are also working on these related projects:

Development of electrochemical systems based on 3D nanocomposite materials (hydrogels / nanoblocks) View project

All content following this page was uploaded by Federico A. Viva on 23 September 2014.

The user has requested enhancement of the downloaded file.

Chapter 7
Carbon Materials for Fuel Cells

Mariano M. Bruno and Federico A. Viva

Abstract Carbon materials are fundamental for the manufacturing of fuel cells. Several fuel cell components are made entirely of carbon in a graphitic form. In the present chapter, an overview of the different fuel cell carbon components and the materials used in their preparation will be presented. Novel approaches in the synthetic method, in order to impart desired properties, and in the manufacturing of the components will be shown. Also, relevant results on the latest research conducted will be discussed.

7.1 Introduction

Fuel cells (FC) are electrochemical devices that convert chemical energy directly into electrical energy and are considered to be the best choice to replace batteries for delivering power for a wide range of applications. The advances made in the basic understanding of fuel cells as well as improvements in fuel cell technology allow us to realize the benefits of switching to fuel cells as reliable power sources.

The main component of a Polymer Electrolyte Membrane Fuel Cell (PEMFC) is the Membrane Electrode Assembly (MEA) [1, 2]. The MEA is formed by a polymer membrane flanked by two electrodes. The membrane acts as the ionic conductor between the two electrodes; the anode, where the fuel is oxidized, and the cathode, where the oxidant is reduced. The electrodes are formed by a porous material named Gas Diffusion Layer (GDL) with a thin layer of an electrocatalyst denominated the Catalyst Layer (CL), The electrocatalyst, responsible of driving

M.M. Bruno (✉) • F.A. Viva
Grupo Celdas de Combustible, Departamento de Física de la Materia Condensada, Centro Atómico Constituyentes, Comisión Nacional de Energía Atómica (CNEA), Av General Paz 1499 (1650), San Martín, Buenos Aires, Argentina
e-mail: mbruno@tandar.cnea.gov.ar; viva@tandar.cnea.gov.ar

H.R. Corti and E.R. Gonzalez (eds.), *Direct Alcohol Fuel Cells: Materials, Performance, Durability and Applications*, DOI 10.1007/978-94-007-7708-8_7,
© Springer Science+Business Media Dordrecht 2014

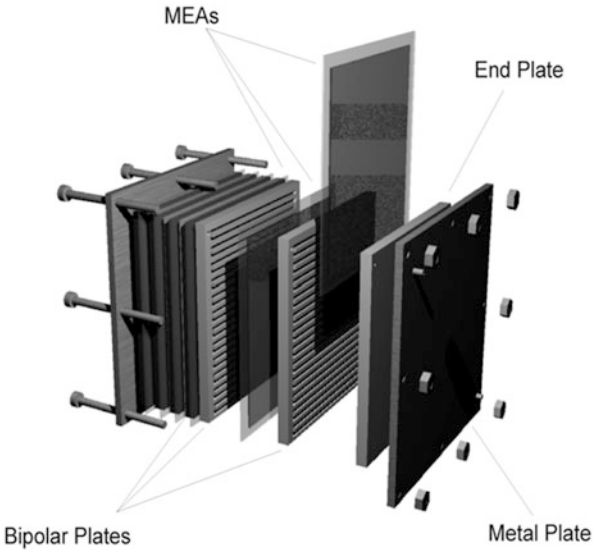

Fig. 7.1 Fuel cell stack components

the electrochemical reactions that takes place at each electrode, is composed by metal nanoparticles (3–5 nm) dispersed on carbon nanoparticles of bigger size (20–40 nm). The GDL–CL combination is commonly referred as gas diffusion electrode (GDE). In a single cell the MEA is placed between a pair of Current Collector Plates (CCP) with channels machined on one of its faces that allows the reactants to flow through the MEA surface. A FC stack is formed by intercalating MEAs with plates machined on both faces (bipolar plates-BP) and contained between two end plates. Figure 7.1 shows a schematic representation of a fuel cell with its different components.

The voltage of a FC is given by [3]

$$E = E_{rev} - \eta_{act} - \eta_{ohm} - \eta_{mass \cdot trsp}$$

Where E_{rev} is the reversible potential, which is the theoretical cell voltage at open circuit conditions. The other three terms represent losses to the voltage known as polarization (η). These are the activation polarization (η_{act}), resistance polarization (η_{ohmic}) and mass transport or concentration polarization ($\eta_{mass\ trsp}$), each of which predominates on a different zone of the polarization plot as shown in Fig. 7.2 and are a function of the current density (j). Under experimental conditions, the thermodynamic E_{rev} is never observed due to irreversible losses such as parasitic electrochemical processes, mixed potentials and even corrosion process [4]. Only the experimental open circuit voltage (OCV) is observed under zero current flow, indicated as E_o in the graph. Apart from the ohmic polarization, related with an energy loss due to the internal resistance of the cell which plays a predominant role on the central part of the plot, the other two polarizations can be divided into contributions from the anode and the cathode. The activation polarization,

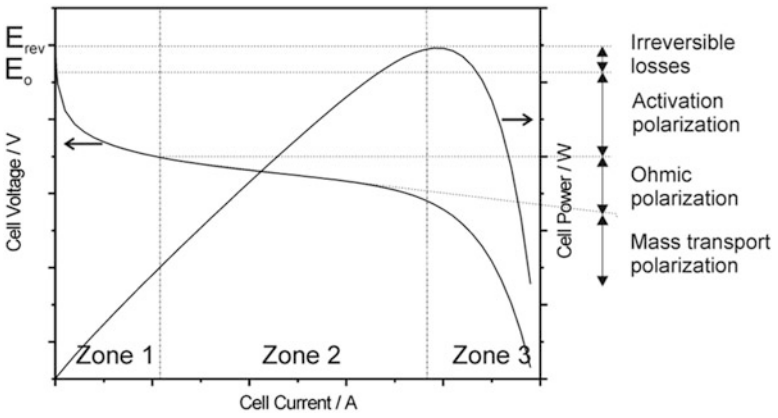

Fig. 7.2 Polarization and power plots and the different polarization contributions

dominant at low current densities, depends on both the chemical nature of the reacting compound and the electrode composition in terms of chemical and physical nature. The mass transport polarization is related to the rate at which the compounds reach the surface of the electrode, therefore it has a dominant contribution at high current densities.

In between the GDL and the membrane, i.e. where the CL lies, emerges a zone denominated the triple phase boundary where the electrocatalyst, the ionic conductor (membrane) and the reactants (liquid or gases) meet. Figure 7.3 shows a simplified representation of the triple phase boundary. In that zone takes place the electrochemical processes that generate the FC voltage an electric current. On the electrocatalyst surface the fuel is oxidized or the oxygen is reduced, the ionic conductor (polymer membrane) allows the H^+ to move from one electrode to the other while the electrons leave or arrive the electrocatalyst through the carbon based conductive material (carbon support, GDL, current collector plate). The properties of the materials involved and the way in which the components are arranged in the triple phase boundary plays a major role in the correct functioning of the FC.

Carbon constitutes the most abundant element of the different FC components. Setting aside the membrane, which is a polymer with a carbon backbone, all the other components, i.e. the CL, GDL and current collector plates (bipolar plates) are made almost entirely of graphitic carbon. The electrocatalyst support of the CL is commonly carbon black in the form of fine powder. GDLs are thin porous layers formed by carbon fibers interconnected as a web or fabric, while current collector plates are carbon monoliths with low bulk porosity. As explained above each of these components has a particular function within the fuel cell and in particular in the triple phase boundary. The structure and properties of the carbon in each of the different FC components will determine the whole performance of the cell.

Cost is a major factor for the implementation of fuel cells in the everyday use [5, 6]. There is some variation in the cost percentages assigned to each component

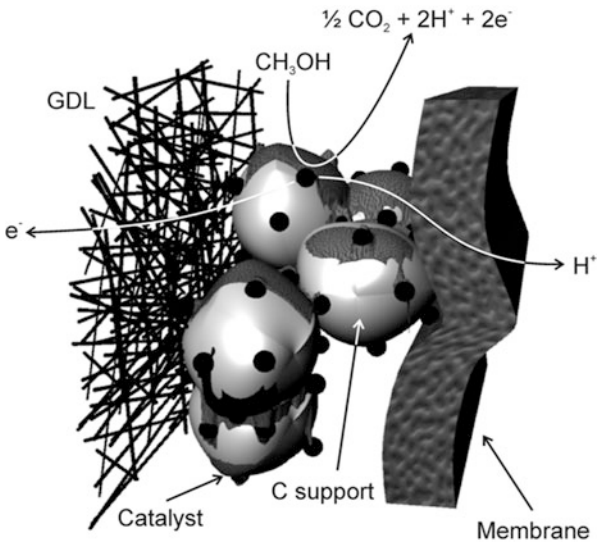

Fig. 7.3 Schematic representation of the triple phase boundary in the MEA

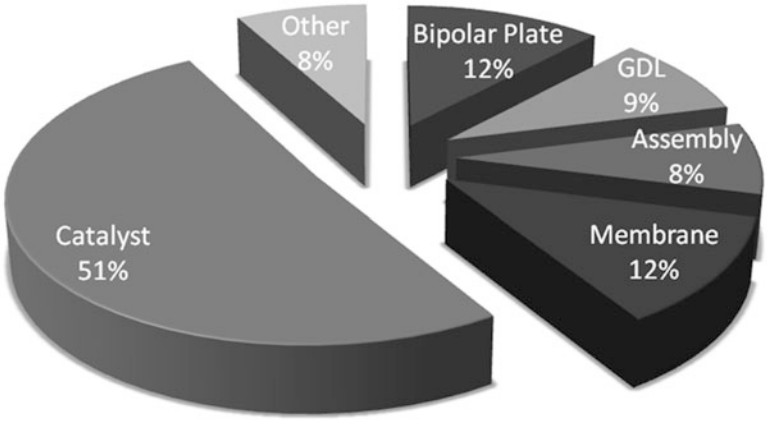

Fig. 7.4 Cost distribution of a fuel cell stack

[5, 7–9] which is related to the kind and size of system considered and to the analysis model used [8, 10]. Figure 7.4 shows the different cost contribution for a FC stack compiled from several sources [5, 9–11]. The bipolar plates and GDL contributes together to 21 % of the stack cost making those components an important factor in the final cost. Reducing the cost of the carbon based components is as important as improving their individual properties.

7.2 Carbon as Catalyst Support

Carbonous materials have excellent properties as support for electrocatalysts in fuel cells. Besides being an electronic conductor with low cost, they possess a good corrosion resistance to acidic and basic environments and low density. In the last decades, the syntheses of structured carbonous materials with controlled and designed properties have taken major attention in the scientist community, where their application can generate a technological advance on energy devices i.e., nowadays the production of carbon materials with tailored physical and chemical properties can help to the developing of power sources devices.

Direct methanol fuel cell (DMFC) suffers some drawbacks which are currently investigated in order to improve their performance and durability, and reducing their cost. In this regard, several approaches are being used to overcome these issues. Among those, can be mentioned [12]:

- Reducing Pt content by developing metallic alloy or Pt-free electrocatalysts.
- Reducing the electrocatalyst loading in fuel cell electrodes by decreasing particle size and avoiding their sintering.
- Increasing mass-transport at the fuel cell.
- Increasing the durability of the fuel cell components.

Porous carbons with tuneable properties have great potential to achieve the goals listed above. An adequate pore size of the carbon support would provide high catalytic dispersion and would enhance the mass transport, which implies a significant cost diminution of the fuel cell by reducing the catalyst loading.

The pore size distribution in the carbon support is an important factor for a well performance of the catalyst. Pores in the nanometric scale are classified by IUPAC in three groups: the micropores are those with diameters lower than 2 nm, the mesopores with diameters between 2 and 50 nm and the macropores with diameters larger than 50 nm. Each pores size offers different benefits, the micropores produce materials with high surfaces area but could be inaccessible to liquid solutions or have slow mass transport. A material with mesopores has a lower surface area but better accessibility than those with micropores. Finally, materials with macropores show the lowest surface area, but they are easily accessible to liquid fuel. For this reason, the structured carbons, principally mesoporous carbon, have attracted considerable attention due to their potential application in the catalyst area, where the challenging is to favour the dispersion of catalyst and allow the accessibility of liquids that feed the anode side of a DMFC. In the following sections a description of different carbons support will be discussed stressing on the effect of the porous structure.

7.2.1 Carbon Blacks

Carbon blacks are produced by pyrolysis of hydrocarbons from petroleum derivatives. Generally, the carbon blacks are composed of spherical nanoparticles that have crystalline domains composed by stacked layers parallel to the surface.

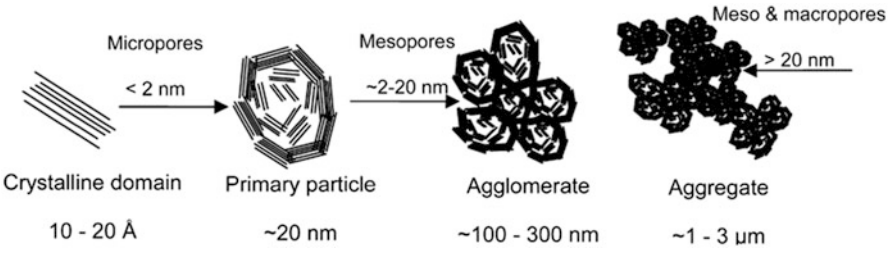

Fig. 7.5 Schematic representation of the structures of carbon black supports: crystalline domain, primary carbon particle, agglomerate and aggregate [13] (Reprinted by permission of the publisher)

This order ensures some degree of graphitization for the materials. The particles are found building aggregates in the form of chains or clusters forming meso and macropores, as show in the Fig. 7.5.

Carbons black includes several types of carbons, such as acetylene black, channel black, furnace black, lamp black. Commonly, their names are referred to the process or the source material from which they are made. Among those, the production of furnace black is the most important. Its production process consists in feeding a furnace with natural gas and aromatics oils as feedstock, where is vaporized and then pyrolyzed. Vulcan XC-72 (a furnace black from Cabot Corporation) is the most widely used catalyst support for low-temperature fuel cells due to their low cost and high availability, being this material used as standard to compare other types of carbons. Vulcan XC-72, formed by nanoparticles of 20–40 nm, has an electrical conductivity of 4 S cm^{-1}, a sulphur content of 0.05 %, and a negligible oxygen content [13]. Within the textural properties Vulcan carbon has a superficial area of 252 m^2 g^{-1}, with a total pore volume of 0.63 cm^3 g^{-1} and a pore size distribution around 15 nm [14].

Like most of the materials (GDL, membranes) used in DMFC, the application of carbon black as catalyst support is a direct extrapolation of their use in hydrogen fuel cell. However, the processes occurring in the anode side are more complex. The carbonous support besides promoting a high dispersion of the catalyst (catalytic area), should allows also the free entrance of the liquid alcohol to the catalyst and avoid the occluding of the gas close to the catalytic zone. Nevertheless the pore structure should not hinder the triple phase boundary formation.

Active sites on the carbon surface, which are unsaturated carbon atoms at the edges planes, defects of the graphitic hexagonal crystallites and oxygen surface groups, provides anchoring centres for catalyst particles favouring the nanoparticle dispersion and inhibiting their sintering [15]. The proportion and nature of these active sites have a strong effect on the preparation, morphology, particle size and catalytic activity of supported catalysts. Fortunately, several authors have been devoted to study the effect of carbon properties on the preparation, dispersion and catalytic activity of supported nanoparticles [16–24]. Takasu et al. [21] analyzed the effect of the surface area of the carbon support on the characteristics of PtRu nanoparticles which were prepared by

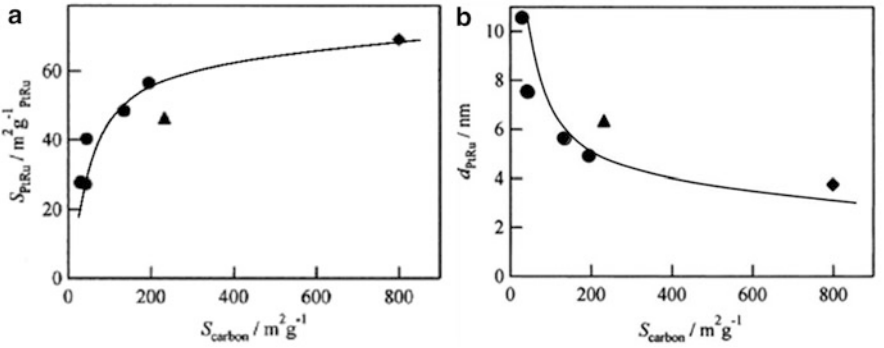

Fig. 7.6 The dependence of (**a**) the specific surface area, SPtRu, and (**b**) particle size, dPtRu, for Pt50Ru50(30 mass%)/C catalysts on the specific surface area, Scarbon, of the carbon black support: ● Mitsubishi, ▲ Vulcan XC-72R, ♦ Ketjen EC [21] (Reprinted by permission of the publisher)

conventional impregnation method. Figure 7.6 a, b show the dependence of the specific surface area of carbon blacks supports, with specific surface area in the range of 29–800 $m^2\ g^{-1}$, on the electrochemical surface area and the particle size of $Pt_{50}Ru_{50}$, determined by CO_{ad} stripping voltammetry and from HRSEM micrographs of the catalysts, respectively. It is important to remark that the increasing of superficial area indicates that a larger portion of the pores is in the size range of micropores.

Carbon blacks as support lead to an increase of electrochemical surface area and a decrease of the nanoparticle diameter of the catalyst when increasing the carbon surface area, at equal synthesis conditions. However, the carbons with higher micropores content did not show a positive effect on the methanol oxidation reaction. Uchida et al. [25, 26] showed for Pt/C that the catalyst structure on the carbon support has a strong effect on the performance of hydrogen fed fuel cells, focusing their analysis in the performance of triple phase boundary. In order to get the optimal microstructure of the catalyst layer they analyzed its components and preparation, reporting that the colloids particle size distribution of the perfluorosulfonate ionomer (Flemion®) in butyl acetate had a mean diameter *ca*. 43 nm. This result suggested that the ionomer colloids could not penetrate into pores < 40 nm and the Pt nanoparticles inside of these pores did not take part of the triple phase boundary. Therefore, a diameter of 40 nm could be considered as the minimum diameter of pore to take advantage of all the catalyst deposited.

A similar study was carried by Rao et al. [23] in Sibunit carbons. They analyzed the pore effect on the performance of DMFC with carbon supports with a range of surface areas from 6 to 415 $m^2\ g^{-1}$. Figure 7.7 shows the observed specific activity for methanol oxidation at an anode potential of 0.5 V as a function of the surface area.

A downward trend of specific catalytic activity when carbon surface area is increased is observed. This behaviour can be attributed to many factors, but the authors emphasized that the particle size (indicated in the labels of Fig. 7.7) and

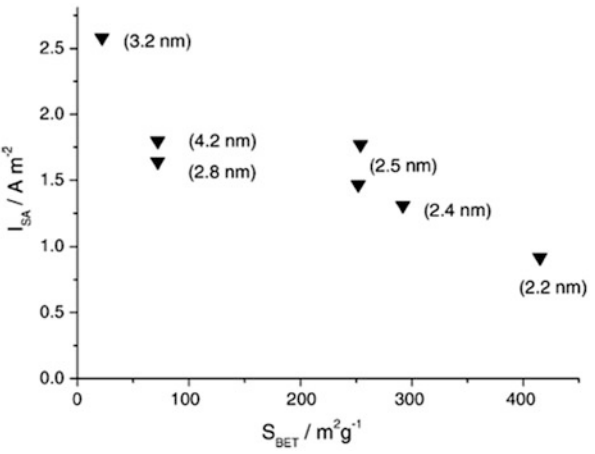

Fig. 7.7 Specific activities (A m^{-2}) at 0.5V RHE plotted versus surface area (SBET) of carbon supports [23] (Reprinted by permission of the publisher)

dispersion of catalyst were maintained almost constant. Moreover, the authors reported a similar trend for catalyst utilisation versus surface area. This trend agrees with those observed by Uchida et al. [26], indicating that the perfluorosulfonate ionomer colloids do not penetrate into the carbon pores of small diameter. However, Rao et al. suggested that with pores size larger than 20 nm optimal results were achieved.

As stated above, high surface area of a carbon support has a positive effect on the dispersion of the catalyst. However, catalyst particles within small pores may not contribute to the triple phase boundary. Therefore, microporous materials should be discarded as catalyst support, while carbons with large mesopores would promote a high electroactive area of the PtRu catalyst and would facilitate the mass transport.

7.2.2 Carbon Nanotubes and Nanofibers

The extraordinary mechanical, electronic and thermal properties of carbon nanofibers (CNFs) and carbon nanotubes (CNTs) make them suitable in several fields of materials technology, including supported catalysts for energy conversion. Graphite nanofibers, carbon filaments and carbon nanotubes, are terms employed to refer to nanofilamentous carbon. These materials can be classified into two categories: fibers and tubes. A schematic representation of their structural features is shown in the Fig. 7.8.

Although, the first report about the production of graphite nanofibers is older than a century [27], the discovery, in 1991, of multi-wall carbon nanotubes (MWNT) by Iijima [28], caused a renewed interest in this kind of carbons. There are several types of carbon nanofibers which differ in the disposition of the graphene layers. In Fig. 7.8 are shown the ribbon-like graphite nanofiber, where the graphene layers are parallel to the growth axis, the herringbone nanofibers having their layers stacked obliquely

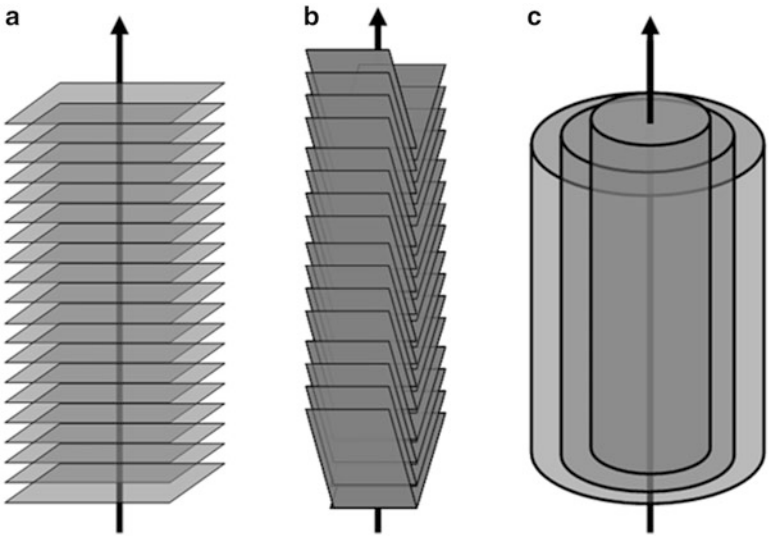

Fig. 7.8 Structure of different types of carbon nanofibers and nanotubes: (**a**) graphitic platelets, (**b**) graphitic herringbone and (**c**) multi-wall nanotube

respect to the growth axis, and the carbon nanotubes composed by graphene layers wrapped around a hollow cavity. Among them, carbon nanotubes have become one of the most active materials under study [29]. The most suitable method to produce them is by chemical vapor deposition. In this versatile process, a gas-phase rich of hydrocarbons are catalytically decomposed at high temperatures.

Carbon nanotubes can be formed by one or several wrapped graphene layers, accordingly they are classified as single-wall carbon nanotubes (SWCNT) or multi-wall carbon nanotubes (MWCNT). Usually, the internal diameter of the tube varies between 2 and 50 nm, the interlayer spacing is *ca.* 0.34 nm and the length ranges from few microns to several millimeters. Pores in MWCNT can be mainly divided into the inner hollow cavities of small diameter and pores (widely distributed, 20–40 nm) formed inside the aggregates of MWCNT. The surface area of MWCNT varies from about 50 to 400 $m^2\ g^{-1}$. The rolled up graphene layer forming the nanotube has a sp^2 hybridization, with structural defects that helps to anchor the catalyst support. In order to increase anchoring sites, many authors suggest different types of activation processes to promote superficial groups or structural defects necessary to have a good fixation of the nanoparticles [17].

Most of the alternative carbons support proposed to replace carbon black still have a lack of test analysis in a fuel cell. However, among those, the carbon nanofibers were the most studied in DMFC. Drillet et al. [30] analyzed the performance of SWCNTs, produced by the arc-discharge method, as catalyst support in the anode side of fuel cell. They used hot air (300 °C) or concentrated nitric acid as activation treatments to promote the catalyst anchoring. The performance of DMFC using SWCNT as PtRu support was 10–15 % higher than those using Vulcan carbon.

In the case of commercial MWCNTs as PtRu support, Jeng et al. [31] used this kind of support previously activated by chemical treatment. Well dispersed PtRu 1:1 nanoparticles of 3.5–4 nm were obtained by a polyol synthesis method. The fuel cell test showed a performance 50 % higher than that of a commercial PtRu on Vulcan support (E-TEK). Similar results were found by Prabhuram et al. [32] for PtRu on oxidized MWCNT, where well dispersed nanoparticles of 4 nm were obtained by the $NaBH_4$ method. The DMFC performance test of PtRu supported on MWCNTs showed a power density *ca*. 35 % higher than that using the Vulcan carbon support. Outstanding results were obtained by Tsuji et al. [33] with PtRu nanoparticles supported on carbon nanofibers prepared by polyol method and tested in a DMFC. They obtained a performance 200 % higher than standard PtRu on Vulcan carbon from Johnson Matthey.

7.2.3 Structured Porous Carbon Materials

The syntheses of materials with tailored properties have been proposed to improve the performance of the fuel cells [12, 34, 35] by increasing the dispersion of the metal, decreasing the formation of agglomerates of catalyst nanoparticles, and raising the diffusion of species from/to the electroactive area. Several synthesis routes produce a carbon with tailored porous structure and composition by controlling the properties of the carbon precursor. The fabrication method to obtain a porous material, in general, can be enclosed in three steps:

This sequence of steps offers numerous benefits to obtain a carbon material with tuneable properties because is possible to introduce modifications, during the procedure of fabrication, depending on the conditions used or the customized steps (one o more) during the fabrication route. It is possibility to get desired characteristics of the final product, such as:

- Controllable carbon composition.
- Controllable graphitization degree.
- Variable surface functionalities.
- Tailored pore size and surface area.
- Tuneable morphology.
- Moldability of monolithic precursors.

In the following sections the most known fabrication routes will be discussed, including:

1. Modifying the drying conditions. The drying condition applied has a strong effect on the final properties of the polymer gel:

- Xerogels: the wet polymeric gel is dried under ambient pressure.
- Cryogels: the gel is frozen and then the solvent is removed by sublimation under low pressure.
- Aerogels: The solvent occluded into the polymer is exchanged with liquid CO_2, which is then removed by using supercritical conditions.

2. Nanocasting-hard template: a rigid structured inorganic template is infiltrated by a carbon precursor to synthesize carbons with uniform pore structure.
3. Mesoporous carbon by soft template: Carbons with mesostructures have been synthesized by using amphiphilic block copolymer as direct template, self-assembly surfactants or polyelectrolytes in the polymerization media of the carbon precursor.

All the above mentioned routes introduce modifications during the synthesis and drying stages. Once the dry structured polymer is obtained, the carbon material is formed by carbonization. During this process the polymer precursor is converted into carbonous materials by heating in an inert atmosphere up to final temperature which is generally above 800 °C. Phenolic polymers are usually used as carbon precursors due to their easy availability, low cost and simple synthesis. These materials have a carbon yield around of 52 % wt at 1,000 °C. An activation process can be performed, during or after carbonization stage, in order to increase the pore volume and the number of superficial groups of carbon materials. However, the activation process is more common in natural carbon precursors than for structured materials.

7.2.3.1 Mesoporous Carbons by Sol-Gel Process: Aerogels, Xerogels and Cryogels

Organics sol-gel refers to the product obtained by a hydrolysis-condensation reaction mechanism. This mechanism is based on a route analogous to sol-gel inorganic oxides. Sol-gel route involves the conversion of a colloidal suspension of a solid in a liquid (sol stage) to a semi-rigid colloidal dispersion (gel stage). The gel is composed by solid and liquid phases, which are independent of each other. If the liquid phase is removed from the gel through a non-destructive manner, a highly porous solid will be left with approximately the same shape and volume as the original gel. The first carbon aerogel, obtained from the carbonization of an organic gel, was produced by Pekala et al. [36] in 1989. The gel was synthesized by polymerization of resorcinol (R) and formaldehyde (F) and dried using supercritical conditions. Briefly, sol-gel reaction in a RF polycondensation occurs through the formation of a gel composed by nanosized pores and polymeric particles highly crosslinked. The polymerization begins with the addition of formaldehyde to the benzene ring, generally activated by basic catalyzers (C). During the second stage, successive condensation reactions produce a polymer highly interlinked. The formation process is schematized in Fig. 7.9.

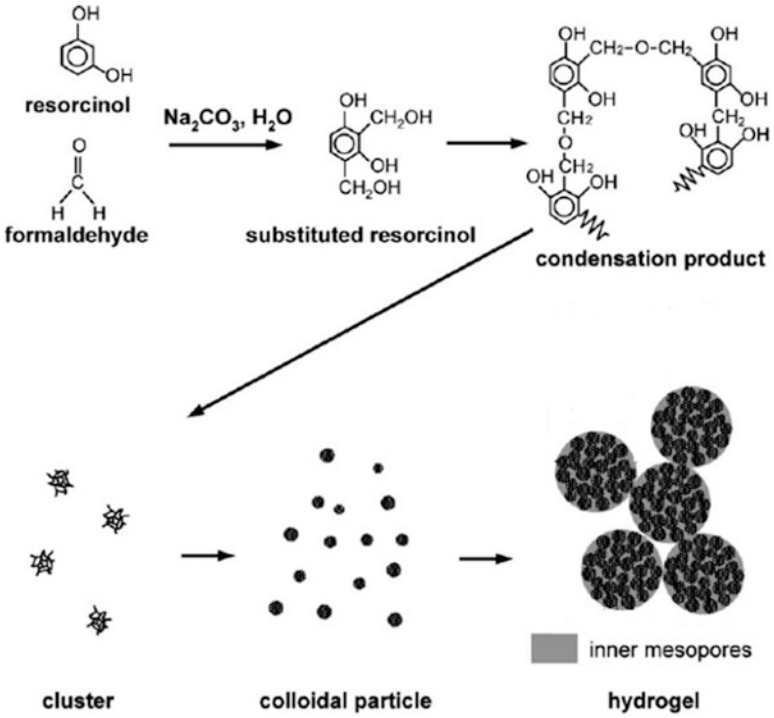

Fig. 7.9 Formation of an organic gel [37] (Reprinted by permission of the publisher)

Although the most common precursors are resorcinol and formaldehyde, the synthesis of polymers by sol-gel method have been extent to others hydroxylated benzene compounds (phenol, catechol, hydroquinone, cresols, phloroglucinol) and aldehyde compounds (e.g. paraformaldehyde, acetaldehyde, furfural) [38]. Moreover, water (W) as solvent and Na_2CO_3 as catalyst have been replaced by other compounds, opening the possibilities to a great variety of materials with different properties [39]. The sol-gel method is a very versatile route and the properties of the gel are strongly affected for the conditions used during its preparation e.g. pH, ratio R/C, reactant concentration, curing time, solvent [37, 40–42]. Since the work by Pekala the organic gels have been extensively studied, analyzing the synthesis route in order to control and tailor the gel properties. In Table 7.1 are summarized some synthesis conditions and the effect produced on the gel properties.

After obtaining the wet gel, it follows a solvent extraction process to dry it. When a gel with low mechanical strength is dried by simple evaporation, capillary forces created at the curved liquid–vapour interface can produce the shrinkage of the pore structure. Therefore, a carbon without appreciable surface area (closed pores) is obtained. For this reason, the drying method has a decisive effect in the structure of material. There are several routes to dry the carbon precursor and each of them produces different change in the properties of material.

Table 7.1 Effect of the synthesis conditions on the properties of resorcinol-formaldehyde carbon gels [43]

Factor	Effect
Decreasing reactant concentration (equivalent to reducing R/F, R/W or R/C)	Smaller particles and pore sizes
	Increases the surface area of xerogels
	Decreases the elastic modulus of carbon aerogels
Acidic catalytic solutions	Low concentrations: small, smooth, fractal aggregates of particles with wide pore size distribution
	High concentrations: no fractal aggregates very narrow pore size distribution
	May reduce gelation time
Alkaline catalyst solution	High concentrations: polymer gel (small polymer particles interconnected with fibrous appearance, high surface area, high mechanical strengths), reduces gelation time
	Low concentrations: colloidal gels (large particles interconnected with narrow necks, low surface areas, low mechanical strengths)
Increasing gel pH	Increases surface area and pore volumes of carbon aerogels
	Insignificant effect on surface area of carbon xerogels
	Increases the pore volume of carbon xerogels at high density of reactants
	Gelation time decreases
Gelation and curing period	Required to improving the crosslinking of the polymer particles
Temperature	High temperatures causes a shrinkage of porosity

If the wet gel is dried at ambient pressure by solvent evaporation as it was describe above, the resulting organic gel is called xerogel. However, in order to reduce the capillary forces which cause collapse of the structure, previously drying, the water can be exchanged by solvents of lower surface tension (e.g. ethanol acetone, etc). Some authors have subclassified these materials in xerogels and ambigels, according to the last solvent evaporated. Ambigels are those materials obtained from hexane or ciclohexane solvent evaporation.

A supercritical condition is other method to suppress the liquid–vapour interface or reduce the capillary forces. This route, used commonly to produce inorganic aerogels, was applied by Pekala et al. [36] to obtain organic aerogels, where the water in the wet gel is exchanged by a solvent soluble in liquid CO_2 (typically acetone), which is removed using supercritical conditions. These materials are called carbon aerogels.

One of the three best known drying methods is sublimation. The initial solvent in the wet gel is exchanged by one with lower density change on freezing and larger vapour pressure than water. After freezing, the solvent is removed by sublimation under low pressure. The so obtained dried gel is called cryogel.

All these methods have advantages and disadvantages. Concerning to the gel structure, supercritical drying is the best method to obtain an unaffected gel

structure, because no appreciable contraction affects the pore structure. However, economical reasons reduce the possibility of this method to be applied at industrial scale.

Few reports were found dealing with the fuel cell performance of PtRu supported on this type of materials as anode in methanol oxidation. A mesoporous carbon dried under ambient conditions was analyzed as anode support in DMFC by Du et al. [44]. PtRu was deposited on a carbon with a pore size diameter *ca*. 11 nm. The same power density of commercial catalyst in single DMFC test was reached using only two third of noble metal used. Calderón et al. [45] synthesized PtRu catalysts supported on carbon xerogels. The carbon supports have high surface area and a pore size distribution centred to *ca*. 16 nm [46]. Well dispersed PtRu nanoparticles of 3.5–4.6 nm were obtained. Although the catalyst formed showed a higher current densities for the MOR than the commercial E-TEK catalyst, its power density in a DMFC single cell test was poorer.

Following the analysis of carbon pore size effect on fuel cell performance, Arbizzani et al. [47] reported DMFC tests for PtRu on mesoporous carbon cryogels. They achieved the best results for the catalyst supported on mesoporous carbon with pore size distribution around 20 nm in diameter. Again, the high surface area is sacrificed to improve the access of the perfluorosulfonate ionomer through the carbon support having bigger pores sizes.

It is important to remark the difference between the performance of catalyst support obtained by using electrochemical cell and fuel cell test. Such a differences were not only found for mesoporous carbons but also for commercial catalysts, indicating that the processing conditions used to form a catalyst layer, such as ink formulation, catalyst deposition method, pressing conditions, etc., have a strong effect in the good performance of fuel cell. Unfortunately, to the best of our knowledge, there is not experimental report analyzing the best conditions for processing the anodic side of a DMFC with catalyst supported on mesoporous carbon.

7.2.3.2 Mesoporous Carbon by Nanocasting

Although the replication method is one of the oldest ones in the human culture, Knox et al. [48] were the first that proposed to synthesize mesoporous carbon by the hard template method. In 1989 they reported the fabrication of porous carbon by using amorphous silica gels as template. However, Ryoo et al. [49] broke new ground for the fabrication of mesoporous carbons with ordered structures from replication of mesostructured silica. After that, an explosive grow in the structured carbons fabrication from replication method started. Ordered Mesoporous Carbon (OMC) is usually synthesized by nanocasting method, which consists in the infiltration of an inorganic hard template, that was produced by a soft template method (*see section below*), with the carbon precursor. The final material is obtained by carbonization of the precursor and the removing of the template. A scheme of the fabrication procedure of mesoporous carbon is shown in Fig. 7.10.

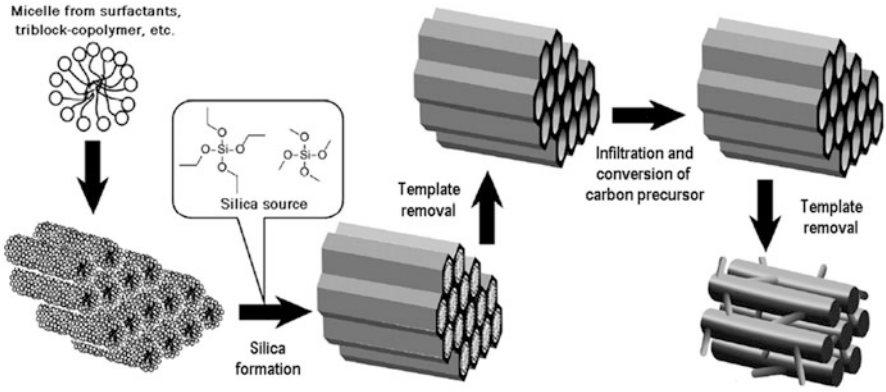

Fig. 7.10 Schematic representation of the synthesis procedures for mesoporous carbon (CMK- · 3) from a mesostructured silica (SBA-15) template [50] (Reprinted by permission of the publisher)

OMCs have been synthesized using various templates, including porous zeolites, and anodic alumina membranes, porous silica materials and silica nanoparticles [51, 52], as well as different carbon precursor: phenolic resins, furfuryl alcohol, mesophase pitch, sucrose, etc. In Table 7.2 are summarized the characteristic of OMC reported in the literature.

A wide variety of carbon with different physical and morphological properties (pore shapes, pore wall thickness, etc.) are reached depending on the template and the carbon precursor used [58]. Moreover, desired properties of the material can be introduced by carbon functionalization [59]. Therefore, a tunable carbon obtained through replication method has a broad spectrum of possibilities that can be used to suit the demand of any system. Among these materials, the structured carbon CMK-3 reported by Ryoo et al. [60] was the most studied as catalyst support in DMFC.

Nanocasting can be considered as the best method to obtain a narrow pore size distribution. This is a very important feature because carbon supports with tunable properties allow the modeling of the system, in order to optimize the processes of methanol oxidation (adsorption and re-dissolution) and mass transport in fuel cells.

For anode in DMFC, Chai et al. [61] used ordered porous carbons with pore sizes in the range of 10–1,000 nm as catalyst support, the material were synthesized using colloidal silica crystalline templates and phenol-formaldehyde as a carbon precursor. They reported a high dispersion of PtRu 1:1 nanoparticles of 2–3 nm on the carbonous materials. Among the catalysts tested, mesoporous carbon with pore size distribution centered on 25 nm showed the best performance in DMFC. Qi et al. [62] also showed that a better performance in DMFC test is achieved by using carbons with higher percentage of pores above 20 nm. Graphitic mesoporous carbons with different surface area, used as PtRu support, were synthesized using resorcinol and formaldehyde and particles of SiO_2 as a template. A power density 24 % higher than that obtained with the commercial PtRu-Vulcan XC-72 was achieved in a DMFC.

Table 7.2 Mesoporous carbons (OMCs) generated by nanocasting

OMC	Space group	Surface area and pore size	Precursor	Template	Space group	Ref.
CMK-1 (SNU-U)	*I41/a or lower*	~1,500 m^2g^{-1} ~3 nm	Sucrose, phenol resin	MCM-48	*Ia3d*	[49]
CMK-2	*Unknow cubic*	~1,400 m^2g^{-1} ~3 nm	Sucrose	SBA-1	*Pm3n*	[53]
CMK-3	*p6mm*	~1,000 m^2g^{-1}	Sucrose	SBA-15	*p6mm*	[54]
CMK-3 analogue	*p6mm*	~3.8 nm	Furfuryl alcohol, phenol resin	HMS SBA-3 MCM-41		
CMK-4	*Ia3d*	~3 nm	Acetylene	MCM-48	*Ia3d*	[55]
NCC-1	*p6mm*	~1,800 m^2g^{-1} ~5 nm	Furfuryl alcohol	SBA-15	*p6mm*	[56]
OMC (cubic)	*Ia3d*	~710 m^2g^{-1} ~6–9 nm	Sucrose, Furfuryl alcohol	KIT-6, FDU-5	*Ia3d*	[57]

OMC carbons obtained from replication of structured mesoporous silicas show a narrow pore size distribution, but with mesopores smaller (< 15 nm) than those obtained from colloidal replication. PtRu nanoparticles supported on ordered mesoporous carbon CMK-3 were analyzed by Din et al. [63] Although a good nanoparticle dispersion was obtained, the catalyst synthesized showed a worse performance than nanoparticles supported on Vulcan XC-72 for methanol oxidation.

Kim et al. [64] analyzed porous carbon by using colloidal silica particles as templates. Carbon with micro, meso and macropores were obtained modifying the initial pH of the carbon precursor solutions. This fabrication method produces materials with narrow pore size distribution in a broad range of pore size. The fuel cell test showed better DMFC performance for carbons with high meso-macropore area with large pore than that with micropores. Again, this effect was attributed to the fact that meso and macropores produce a favorable dispersion of PtRu metal species and allow the access of perfluorosulfonate ionomer for the formation of the triple phase boundary.

7.2.3.3 Mesoporous Carbon by Soft Template

A soft template route involves an organic compound, such as polymers or surfactants, which is used as a direct mold in order to obtain a structured carbon precursor. Then, the soft template is eliminated during the carbonization stage. Nowadays, there are a large number of preparation methods reporting materials with a wide variety of structures and pore size distributions. In general, these methods are more versatile and cheaper than nanocasting ones. Moreover, the

soft template route eliminates steps on the carbon fabrication, because avoids the use of hard template and consequently the chemicals (HF or NaOH) to remove it.

The soft templates are organic compounds able to produce supramolecular arrangements by self-aggregation. The most commonly used are block copolymers and surfactant. The organic template self-assembles forming ordered structures which, through phase separation (nanoscale) and structure stabilization, induce the pore formation in the carbon precursor. Soft template pathways are very dependent of the synthesis conditions (template, solvent, temperature ionic strength, drying conditions, etc.), and this makes them less predictable than the nanocast pathways [65]. The family of phenolic resins are the most used common carbon precursors [66].

Bell et al. [67] were one of the pioneers in proposing the fabrication of mesoporous carbon by using surfactants as template. This novel route produces mesoporous carbon monolithic using directly cationic micelles as nanomolds in the polymerization media. More recently, Fujikawa et al. showed a possible route to control the morphology of the polymer and carbon nanostructures [68, 69].

All authors conclude that carbons with adjusted pore size distribution in the entire range of the nanopores can be obtained, depending the synthesis conditions and cationic surfactants used as templates. Despite this, it is an effective pathway to obtain porous carbons, even though the pore formation mechanism is not well understood. Hence, different mechanisms are used to explain its effect emerged, such as liquid crystal templating mechanism, cooperative self-assembly, electrostatic interaction between cationic surfactant molecules and the anionic RF polymer chain and micelles as nanoreactors to produce RF nanoparticles [51, 70]. In these cases, the simple mold effect from the globular form and the RF polymerization around it is insufficient to explain the structuring of the material by the template, where spherical closed pores would be expected.

Earlier reports showed that with a low surfactant concentration, enough for micelles formation but without reaching the liquid crystalline phase, a porous material with open structure may be obtained [71]. The authors suggested that the cationic micelles around polymeric clusters produce their stabilization and avoid the collapse during the drying step.

Soft template method by using block copolymers was reported for first time by Liang et al. [72] in 2004. After that, a significant progress on the fabrication of carbon with a well ordered mesopores was achieved [32, 73–77]. Zhao and coworkers performed a widespread study of soft template via the triblock poly (ethylene oxide) (PEO) and poly(propylene oxide) (PPO) based systems, PEO-PPO-PEO [65, 78]. Several ordered pore structures corresponding to various surfactant liquid crystal phases were synthesized by liquid crystal template pathway, a schematized synthesis procedure is shown in the Fig. 7.11.

The procedure was divide in five steps: (1) the preparation of resol precursors, (2) the mixed of carbon precursor with triblock copolymer and formation of ordered structure by self-assembly of the block copolymer, (3) the thermopolymerization of the carbon precursor around the template, (4) the removal of the template by calcination, and (5) the carbonization of the carbon precursor.

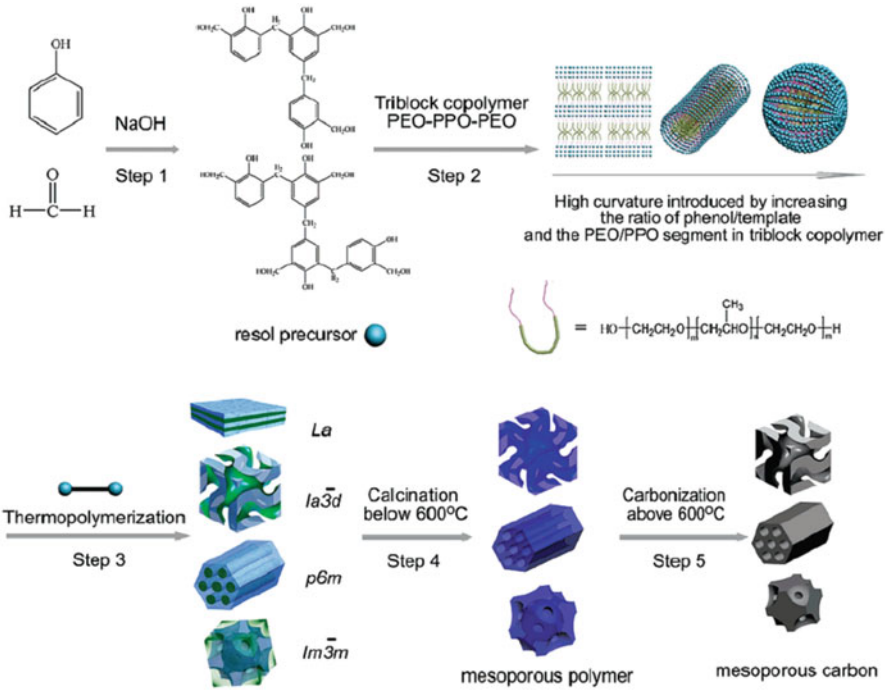

Fig. 7.11 Scheme for the preparations of the ordered mesoporous polymer resins and carbon frameworks [78] (Reprinted by permission of the publisher)

In general, carbons with narrower pore size distribution are obtained by using block copolimers than the ones from cationic surfactant. However, in general their pore sizes are smaller than 12 nm using commercial block copolymers. Deng et al. [79] reported the synthesis of ordered mesoporous carbons with large mesopores by using laboratory-made poly(ethylene oxide)-b-polystyrene (PEO-b-PS) diblock copolymers as templates. Bruno et al. [71, 80, 81] show alternative preparation method to form large mesopores. They found that polyelectrolytes also act as mesopores former, reporting carbons with mesopores size from 8 to 60 nm without ordered structure. Furthermore, these materials have a broader pore size distribution than those obtained by using block copolymers.

As it was discussed above, the carbon with small mesopores used as support produce high dispersion of the PtRu nanoparticles. However, in the fuel cell test they can show a poorer performance than the catalysts supported on Vulcan. Catalyst nanoparticles deposited in a tight pore might be unconnected to the perfluorosulfonate ionomer and inaccessible to the methanol. However, other factors affect the triple phase boundary and in consequence the performance of the cell using small mesopores carbon supports. For example, the method of catalyst layer formation, including ink formation and dispersion of the catalyst

over the anode side, is a key factor in order to increase the fraction of catalyst contributing to the triple phase boundary region.

Viva et al. [82] synthesized PtRu 1:1 nanoparticles on mesoporous carbon and Vulcan carbon by using an impregnation method. The mesoporous carbon, obtained by using polyelectrolyte as structuring agent, had a surface are of 580 $m^2\ g^{-1}$ and a broad mesopores size distribution with a maximum centred at 20 nm. TEM images show the formation of highly dispersed nanoparticles of *ca*. 4 nm. PtRu nanoparticles exhibited a better methanol efficiency conversion when supported on mesoporous carbon as compared to Vulcan, and also showed an improved fuel cell performance. These results are in agreement with those showed by Chai et al. [61] where carbons with the larger mesopores exhibit the best cell performance.

7.3 Gas Diffusion Layers

As it was described in the introduction one of the many components of the MEA is the gas diffusion layer. The roles of the GDL are multiple and described below:

- Provides an even distribution of the reactants throughout the CL and the elimination of water and products (CO_2) out of the cell.
- Provides a substrate for the catalyst, present in the form of a powder. Also avoids deformation of the membrane-CL from the channels machined on the CCP.
- Provides the electrical connection between the CL and the CCP allowing electrons flow to/from the load.
- Transfers the heat generated on the catalyst away from the MEA.

The tasks mentioned above demands a particular set of properties for the compounds conforming the GDL: good mechanical properties, good porosity for the inlet and outlet of the reactant and products, good electrical conductivity and good thermal conductivity. The most widely used materials for GDLs is carbon in the form of carbon fibers, which is commercially available in the form of paper or fabric. It is worth to mention, even though they will not be discussed in this chapter, that metal meshes and porous metal foils are also used as GDL [83].

7.3.1 Carbon Fibers

Carbon fibers (CF) are known since the late 1800s. Thomas Edison produced the first carbon fibers from the pyrolyzation of bamboo and cotton fibers for the light bulbs filament. The fibers sustained high temperatures although they lacked tensile strength. The development of modern carbon fibers began in 1960 when Shindo produced the first carbon fiber from the pyrolysis of polyacrylonitrile (PAN) [84, 85]. Other materials also used for CF fabrication are rayon, phenolic resins and pitch. The CF properties like; high modulus, high tensile strength and low weight

produced the widespread in the utilization of carbon fibers for a vast range of applications. In particular CF based composites possess excellent mechanic properties which are ideal for a wide range of applications particularly ones where a light and strong material is needed such as in airplanes, cars, boats, aerospace, sporting goods, etc.

The CF fabrication starts with the formation of PAN fibers by a spun process, from a solution or suspension of acrylonitrile, a co-monomer such as methyl acrylate or methyl methacrylate and a catalyst in a solvent like dymethylformamide. The most common spinning processes to form the fiber are: dry spinning, where the fibers are form in drying chamber while the solvent evaporates, and wet spinning where the fibers are form in a coagulating bath. Another method used to spun fibers is electrospinning which allows the formation of fibers a few nanometers in diameter [86, 87]. In the electrospinning method a potential difference is applied between a syringe needle and a surface where the fibers will be collected.

Once the fibers are formed they go through a stretching process where the polymer chain aligns and orientates parallel to the fiber longitudinal axis. An elongation of 500–1,500 % occurs contributing to the high strength of the final CF. The fiber might be subjected to a modification process previous to the pyrolysis which might include resin coating, chemical impregnation and stretching with plasticizer. Modification of the fibers affects the pyrolysis process by reducing the activation energy of cyclization reactions, decreasing the stabilization energy, and also improving the orientation of molecular chains in the fibers [88, 89]. The fibers are then subjected to the pyrolysis processes which has different stages depending on the type of CF desired [89]. Figure 7.12 shows a schematic representation of the pyrolysis process and the types of fiber obtained. The first stage is termed stabilization where the fibers are heated between 180 °C and 300 °C in the presence of air for 30–120 min. The working temperature depends on the manufacturer. In this stage there is a change from the linear atomic bonding to a more thermally stable ladder bonding [90] (i.e., thermoset material), by a reorganization of the bonding patter through the uptake of oxygen molecules from the air [91]. The next stage is either carbonization or graphitization, depending on the temperature, by heating the stabilized fibers in an inert atmosphere. The temperature used will define the properties of the final fiber. Carbonization up to 1,300 °C will produce Type III CF, which presents low modulus and low tensile strength. For temperatures of 1,500 °C Type II CF are obtained with high tensile strength and medium modulus. For temperature above 2,500 °C (graphitization) Type I carbon fibers, with high modulus and low tensile strength, are obtained [90, 92].

7.3.2 Carbon Paper

Carbon paper (CP) preparation begins by chopping carbon fibers obtained between 1,000 °C and 1,400 °C. Typical fiber diameter is between 5 and 15 μm. The porosity of the final product will depend on the length of the chopped fibers: short fibers will render a small pore size. The chopped fibers are soaked in water and a binder,

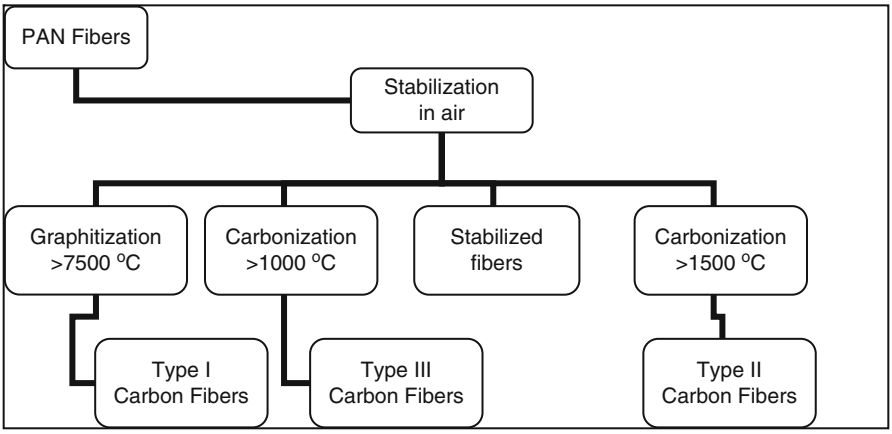

Fig. 7.12 Stages in the carbon fiber pyrolysis process from PAN fibers

typically polyvinyl alcohol [93], followed by a drying step. The coated fibers are impregnated with a resin and subjected to a pre-curing step at 150–175 °C [94]. A number of resins can be used, being the phenolic resin the most common because of its carbon structure, good adherence, and its low cost [94, 95]. The final properties of the CF will depend on the amount of the phenolic resin used [95, 96]. The material with the resin coating is molded into sheets by applying pressure and several sheets can be piled and re-pressed for a thicker material. The sheets are then cured in an oven at 150–200 °C for at least 2 h [96]. After curing, the carbonization and graphitization steps take place. The temperatures and the heating rate are different depending of the manufacturer, therefore modifying the CP final characteristics. As an option, carbon black or graphite powder can be added to the resin before impregnation of the CF improving the electrical conductivity without the need of the carbonization and graphitization steps [95].

In 1970 Toray Inc. was awarded the license of Shindo's patent [85] and started production of CF in 1971. Nowadays Toray is the world largest producer of CF and the Toray CP is one of the most referenced in the literature. Table 7.3 shows the properties of Toray CP. Figure 7.13 shows SEM micrograph of Toray CP TGP-H-060 where the morphology of the CP can be clearly observed.

7.3.3 Carbon Cloth

Carbon cloth (CC) is another kind of GDL used for PEM fuel cell application. Typically carbon cloth is thicker than the average carbon paper but has the important advantage of being flexible. Regarding the through plane electrical

Table 7.3 Physical properties of different types of Toray CP [97]

Product name	Thickness (mm)	Electrical resistivity (mΩ cm)		Thermal conductivity (W/m K)			Gas permeability (ml·mm/(cm^2·hr·mmAq)	Porosity (%)	Bulk density (g/cm^3)	Surface roughness (μm)	Coefficient of thermal expansion (in plane) (25~100 °C) ($\times10^{-6}$/°C)	Flexural strength (MPa)	Flexural modulus (GPa)	Tensile strength (kgf/cm)
		Through plane	In plane	Through plane (room temp)	In plane (room temp)	In plane (100 °C)								
TGP-H-030	0.11	80	–	–	–	–	2,500	80	0.40	8	−0.8	40	8	–
TGP-H-060	0.19	80	5.8	(1.7)	21	23	1,900	78	0.44	8	−0.8	40	10	5
TGP-H-090	0.28	80	5.6	(1.7)	21	23	1,700	78	0.44	8	−0.8	40	10	7
TGP-H-120	0.37	80	4.7	(1.7)	21	23	1,500	78	0.45	8	−0.8	40	10	9

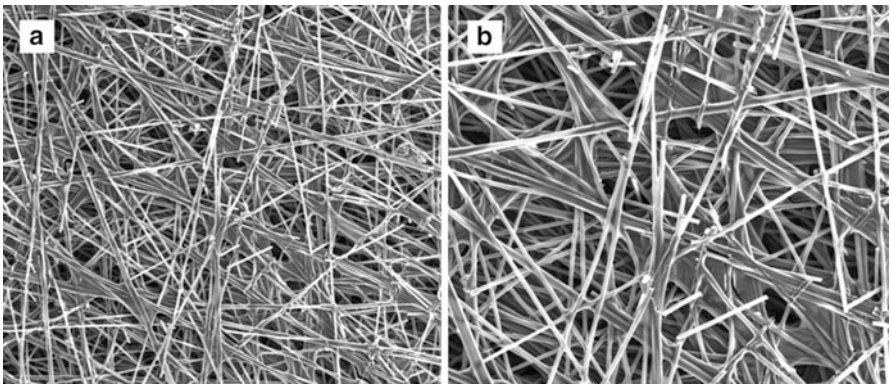

Fig. 7.13 SEM images of Toray TGP-H-60 carbon paper at 200× (**a**) and 400× (**b**)

Table 7.4 Physical properties of different carbon cloth GDL [98]

Product name	Thickness (mm)	Weight (g/m^2)	Bulk density (g/cm^3)	Porosity (%)	Tensile strength (MPa)	Through-plane air permeability (sec/100 cc)	Through-plane resistivity ($m\Omega\ cm^2$)
1071HCB Ballar	0.356	123	0.35	–	–	1.3	7.7
2002HD Ballar	0.229	96	0.42	–	–	2.6	7.2
Elat LT1400w NuVant	0.454	250	0.8	31	–	10	2 (bulk)

conductivity, in average the CC has higher values than CP with the exception of the ones manufactured by Ballard [98] as shown in Table 7.4.

Fabrication of CC begins after the PAN fiber stabilization step. With the stabilized fiber a spun yarn is formed. The yarn is put in a stretch-breaking machine, of common use in the fabric industry, which produces a fiber tow of certain lengths in a continuous way. The yarn is then homogenized with the use of different machines and subsequently braided or directly weaved. Once the cloths are ready, they are heated between 1,000 °C and 2,500 °C (carbonization or graphitization) under an inert atmosphere. As for the CP, the final temperature and heating rate will depend on the desired properties [99, 100].

Figure 7.14 shows SEM micrograph of Ballard carbon cloth while Table 7.4 shows the properties of some commercial CC.

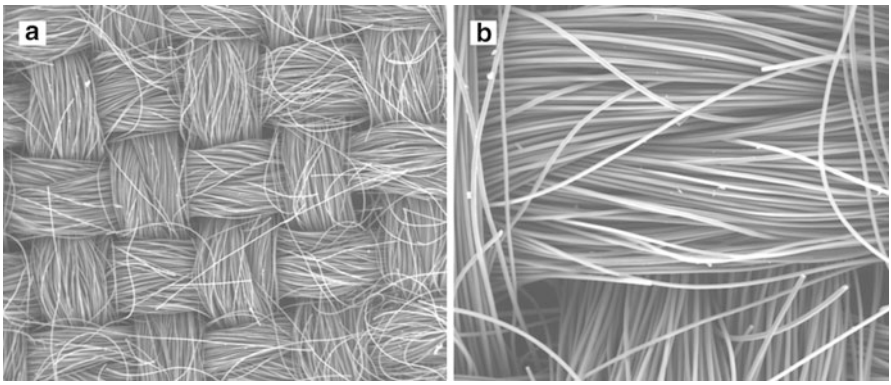

Fig. 7.14 SEM images of Ballard carbon cloth at 200× (**a**) and 400× (**b**)

7.3.4 Carbon Felt

Carbon felt is another kind of CF arrange, generally used as thermal insulation in inert and vacuum furnaces, and that has seen its use in the fuel cell area only in microbial fuel cells (MFC) [101].

7.3.5 Diffusion Layer Coatings

In order to improve the properties of the aforementioned GDLs, they can be further modified by different coatings. These are mainly: treatment with polytetrafluoroethylene (PTFE) and/or the deposition of a microporous layer (MPL) on the face at which the catalyst will be added [102].

7.3.5.1 PTFE Treatment

PTFE treatment of the GDL is one method to control internally the water content. Water management in PEM fuel cells is a key factor for the correct functioning of the device. Water management refers to the control of the water content inside the fuel cell. Low amounts of water within the boundaries of the MEA causes the membrane to dry, consequently reducing the ion transport properties. On the other hand, excessive amount of water particularly on the cathode side, known as cathode flooding, hinders the reaction on the catalyst surface. Both high and low water content may produce the shutdown of the cell. In direct alcohols fuel cells (DAFC), the water management is a key factor because as the fuel is introduced as an aqueous solution the amount of water inside the cell could be excessive.

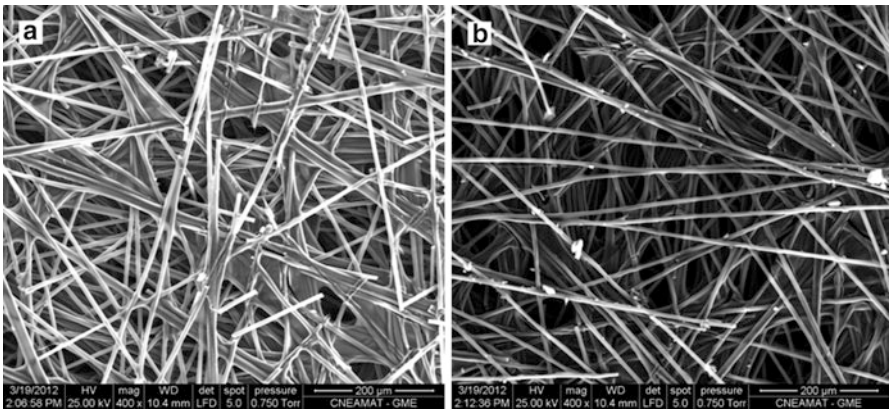

Fig. 7.15 SEM images of Toray TGP-H60 10 wt% PTFE treated (**a**) and untreated (**b**)

The GDL is simply coated with a thin layer of PTFE which renders the material hydrophobic. The coating procedure uses an aqueous suspension of PTFE with a nonionic surfactant such as polyoxyethylene alkyl phenyl ether or polyoxyethylene alkyl ether. The GDL material is soaked in the suspension or it is applied by spraying, this step is repeated according to the desired PTFE coverage. The GDL is then dried in air at temperatures below 200 °C and finally sintered at *ca*. 350 °C for 30–45 min [103, 104]. GDL with different amounts of PTFE are available ranging from 5 % to 30 % where an increased content means higher hydrophobicity. The hydrophobic surface expels the water coming to the anode or through the membrane and prevents condensation of water coming in the gases stream [105]. However, a higher amount of PTFE increases the contact resistance [106]. Moreover, the sintering temperature has been seen to adversely affect the conductivity [107]. Figure 7.15 shows the SEM micrograph of Toray TGP-H60 with 10 % of PTFE treatment and without treatment. The treated paper shows a lighter image due to the decreased electrical conductivity.

Several authors have shown the fuel cell performance with varying PTFE content [103, 106, 108, 109]. Figure 7.16 shows the polarizations curves of DMFC with different contents of PTFE on the anode and cathode GDL respectively [82]. An excess of PTFE has an adverse effect on the fuel cell polarization as observed in both graphs. The better performance is attained with different PTFE amounts at the anode and the cathode, indicating that an optimum amount has to be chosen according to the particular material and application. This is related to the fact that different amounts of water are present in the anode and the cathode. While an aqueous solution is fed to the anode, water reaches the cathode mainly by transport from the anode through the membrane, because dried O_2 or air is typically supply to the cathode.

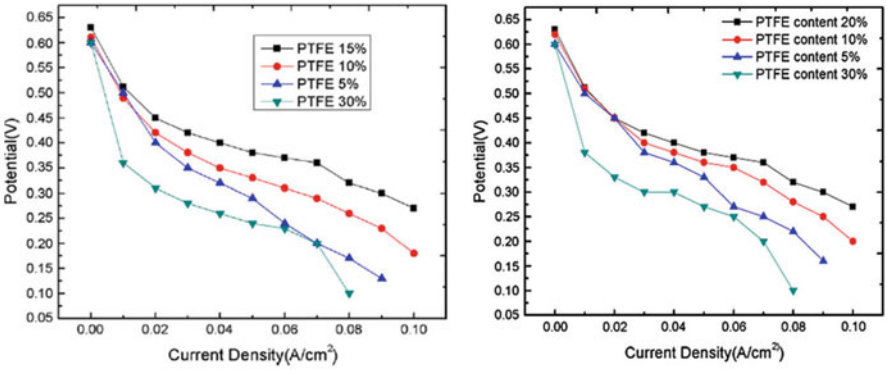

Fig. 7.16 Effect of PTFE content on the anode and cathode backing layer in the performance of DMFC [82] (Reprinted by permission of the publisher)

7.3.5.2 MPL Coverage

The coverage of the GDL by a carbon MPL is another common treatment in order to modify the layer properties. The MPL consist of a thin layer of carbon black powder with PTFE as binder, which is applied on one face of the GDL. Fabrication starts by preparing a slurry of the carbon powder and PTFE in an alcohol solution, typically isopropanol. The GDL is then coated with the mixture either by brushing, spraying, screen printing or with a doctor-blade system. The material is then dried at ca. 80–120 °C for 1 h followed by another heating step at 280 °C, in order to remove the PTFE dispersion agent, and finally sintered at 350 °C for 1 h. MPL thickness varies from manufacturer to manufacturer but typically lay in the order of 5–10 nm. The MPL coverage reduces the surface porosity of the plain CP or CC. Covering of the GDL by the MPL renders pores in the order of 20–200 nm, when in comparison without coverage the GDL pores range between 0.05 and 100 μm [110]. As the catalyst is applied on the MPL side, the pore size reduction effect is quite important because it prevents penetration of the catalyst particles deep into the GDL since the support catalyst particle sizes are between 40 and 80 nm. Thus, the MPL keeps the catalyst layer on the surface of the electrode improving the contact with the membrane and avoiding clogging of the GDL. As PTFE is used for the MPL preparation, this is another option for water management in the MEA. Figure 7.17 shows SEM images corresponding to both sides of Ballard's AVcarb 2240, a flexible carbon paper with a MPL, recommended by Ballard for DMFC applications. The image clearly shows the low porosity of the MPL covered face.

Wang et al. [111] presented a thorough study of MEAs for DMFC prepared with different loadings of Vulcan XC-72 as MPL. Polarization and power plots were obtained with 1.5 M methanol as fuel and humid air (50 % RH) as oxidant. The results (Fig. 7.18) show that 1 mg cm^{-2} of carbon as MPL at the anode or the cathode presents the highest power density when compared to 0.5 and 1.5 mg cm^{-2}

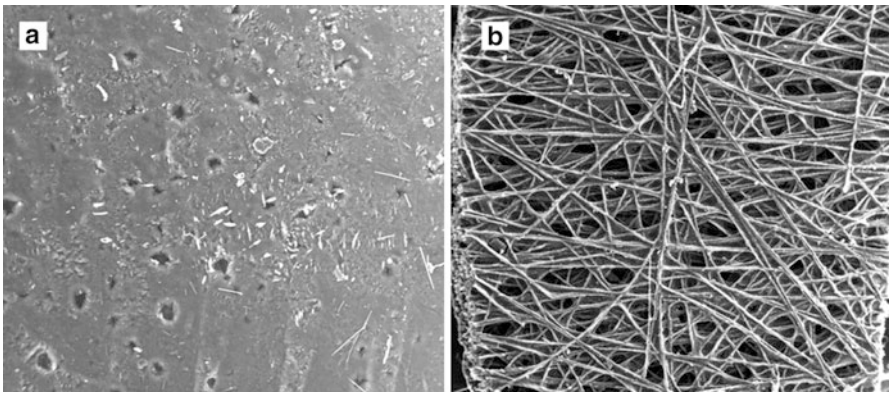

Fig. 7.17 SEM images of both faces of Ballard AVCarb 2240. (**a**) MPL covered face. (**b**) Non covered face

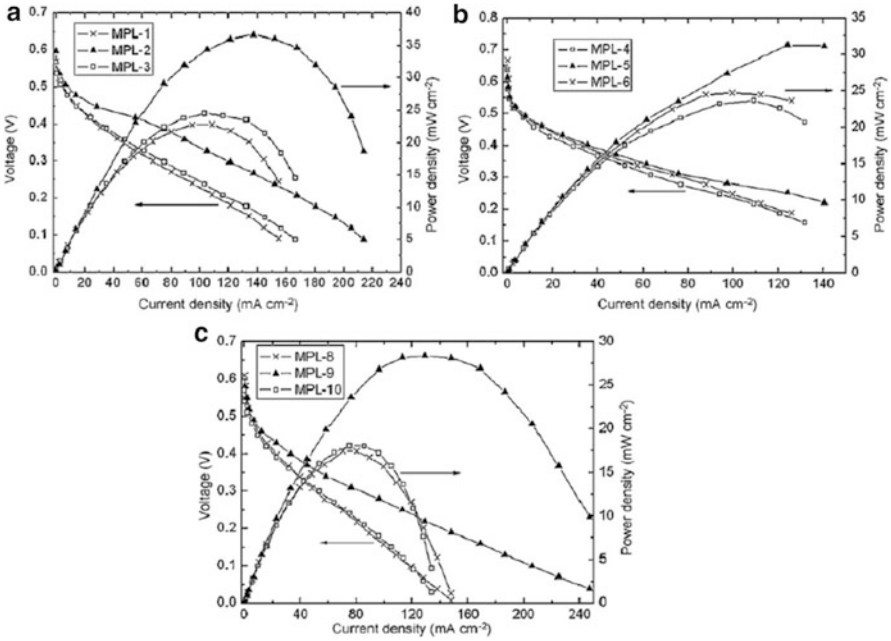

Fig. 7.18 Influence of different carbon loadings on DMFC performance at 35 °C and atmospheric pressure. (**a**) Anode: without the microporous layer, cathode: 0.5 (MPL-1), 1.0 (MPL-2) and 1.5 mgcm^{-2} (MPL-3) Vulcan XC-72 carbon with 20 wt% Teflon; (**b**) anode: 0.5 (MPL-4), 1.0 (MPL-5) and 1.5 mg cm^{-2} (MPL-6) Vulcan XC-72 carbon with 20 wt% Teflon, cathode: without the microporous layer; (**c**) anode and cathode with: 0.5 (MPL-8), 1.0 (MPL-9) and 1.5 mg cm^{-2} (MPL-10) Vulcan XC-72 carbon with 20 wt% Teflon [111] (Reprinted by permission of the publisher)

loadings. On a different MEA the same loading of 1 mg cm^{-2}, both at the anode and cathode, also presents the highest power density. The authors claim that an intermediate loading of Vulcan gives the best electron conduction and mass transfer while the lowest and highest loading had a diminished electron conduction and mass transfer respectively.

7.3.6 Non Commercial GDLs

In the previous section, an overview of the most common commercially available GDLs has been discussed. However, a great deal of research has been conducted on further modifications of commercial GDL or the preparation, at laboratory scale, of GDLs with particular properties. CP and CC processes produces material with low control of the porosity. Mainly, the preparation of non commercial GDLs aims to improve the porosity control in order to obtain a better diffusion of fuel and oxygen and for water management.

Yang et al. [112] prepared GDL with carbon black and PTFE. The layers were like a standalone MPL with high gas permeability. However, the cell performance was half of the commercial materials although the authors stressed the low cost and simplicity of preparation.

Carbon nanotubes (CNT) were used by several researchers to modify commercial GDLs [113–116]. Wang et al. [116] grew CNTs directly over CC by microwave plasma-enhanced chemical vapor deposition using $CH_4/H_2/N_2$ as precursors for DMFC. They deposited PtRu nanoparticles by a sputtering method, obtaining a loading of 0.4 mg cm^{-2}. The anode high performance was attributed to the high conductivity and low interfacial resistance of CNT.

Gao et al. [117] went further and prepared GDL made entirely with CNT. They mixed PAN CF, CNT and PTFE and sintered the mixture at 340 °C for 30 min. The prepared GDL was compared against Toray TGP-H-60 and they observed better electrical conductivity and mass transport properties by electrochemical impedance spectroscopy (EIS). Polarization plot also exhibited a better performance as show in Fig. 7.19.

Gerteisen et al. [118, 119] modified the GDL by drilling holes across it. The holes having 80 μm in diameter were drilled with a laser along the channels of the current plates. As the in-plane water saturation is higher than the through plane, it is expected that holes through the GDL will help in the fast evacuation of water from the GDL/membrane interface. The authors showed an improvement in the fuel cell polarization. In a similar work, Mench and coworkers [120] drilled 300 μm holes on GDL with MPL using also a laser. However, the holes were drilled in an array along the whole GDL surface equally spaced in the XY direction. The authors observed a lower performance compared to non-drilled material with low and very high humidity. Figure 7.20 shows a schematic representation of the differences in liquid water transport within a GDL with and without macro holes. Without water transport channels (WTC) the O_2 path through the GDL to the catalyst might be

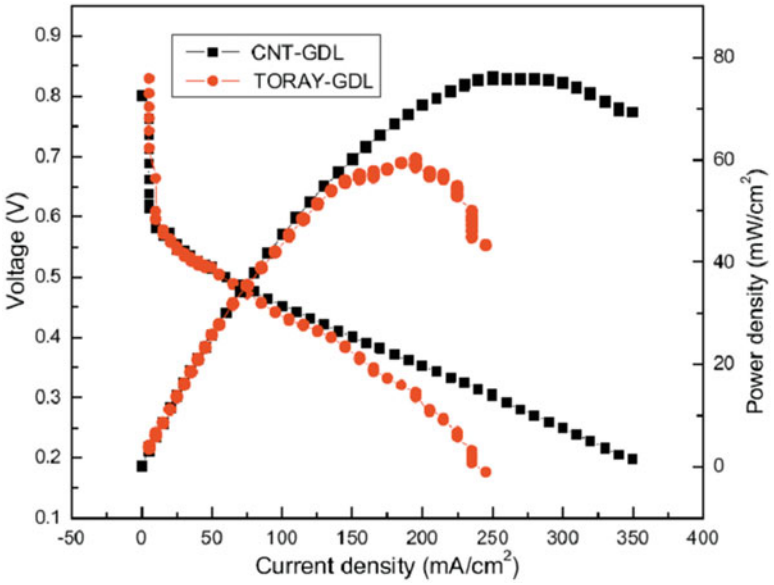

Fig. 7.19 Fuel cell performance comparison at 60 °C for a CNT GDL against a Toray GDL. Anode operation conditions: 1.0 M methanol at 1 ml min^{-1}. Cathode operation conditions: ambient pressure air at 80 ml min^{-1} [117] (Reprinted by permission of the publisher)

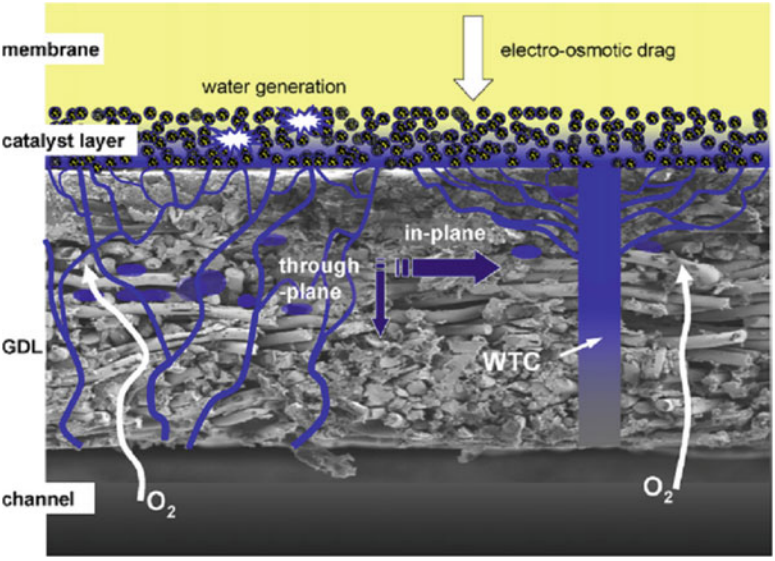

Fig. 7.20 Schematic of the liquid water transport with and without water transport channel (WTC) [119] (Reprinted by permission of the publisher)

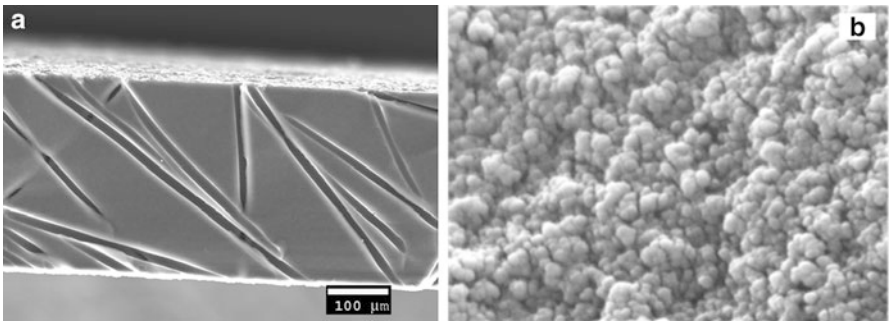

Fig. 7.21 SEM images of a mesoporous carbon monolith. (**a**) Transversal cut showing the through plane channels. (**b**) Surface close up

hindered by water moving in the opposite direction. On the other hand, with WTC the water exits through the transport channels leaving a more open path for the O_2 transport.

The aforementioned results were very promising in order to improve the fuel cell performance. Working in a similar idea, Bruno et al. [81, 121] presented a novel method to produce mesoporous carbon monolith, obtained by a soft template method, with channels in the through plane direction of the materials using polypropylene fibers as a hard template. This simple method produces channels, 15 µm in diameter, together with meso and micropores in a single carbonization step of the resorcinol-formaldehyde resin used as precursor. Figure 7.21 shows SEM images of a transversal cut of the monolith exhibiting the macroscopic capillaries and the material surface showing the carbon particles forming the monolith. This material was later used as GDL and support of a electrodeposited mesoporous Pt catalyst for the anode in an H_2 fed fuel cell [122]. The observed results showed a better performance of the GDL/catalyst combination as compared to the commercial GDLs and catalyst.

7.4 Current Collector Plates and Bipolar Plates

The final component of a fuel cell to be discussed in this chapter is the current collector plates (CCP) or more commonly called the bipolar plates (BP) or flow field plate (FFP). As observed in Fig. 7.1 the fuel cell stack is composed by a number of BP, each of which will separate a pair of MEA and with two end plates completing the stack. At either side of the BP, an arrange of channels provide the flow paths for the fuel and oxygen. One of those faces is in contact with the anode of one MEA and the other face with the cathode of the other MEA, hence, the name bipolar plate. The end plates have channels only on one face, and the stack is typically completed by two metal plates with a series of bolts that holds the stack

Table 7.5 DOE technical targets for bipolar plate [123]

Property	Value
Flexural strength[a]	≥25 MPa
Contact resistance (at 140 N cm^{-2})	<20 mΩ cm^2
In-plane electrical conductivity	>100 S cm^{-1}
Thermal conductivity	>10 W $(m\ K)^{-1}$
Gas permeability	$<2 \times 10^{-6}$ cm^3 cm^{-2} s^{-1} at 80 °C and 3 atm.
Corrosion resistance	<1 μA cm^{-2}

[a]Using ASTM C651 – 11 Standard Test Method

tight. The shape and size of the channel's pattern will depend mainly on the application and final size of the stack. The BPs are the major contributor of a fuel cell stack in weight and volume, accounting for about 60–80 % of the total weight [9].

The BP functions are:

- Distribute the fuel and oxidant uniformly across the GDL outer surface
- Conduct the electrical current from the MEA to the load
- Remove the heat from the MEA
- Remove the reactants in excess and products formed
- Provide the structural support for the MEAs and sustain the compression
- Prevent, along with the seals, reactants or products leaks

Some of these functions are similar to the ones of the GDL and although the main component is also carbon material, the processes to obtain GDL and BP do differ.

Table 7.5 shows the target values of the BP properties set by the US department of energy (DOE) and taken as the goal by researcher and manufacturers.

Carbon is also the main material used for BP. As in the case of GDLs, metals were also used in the fabrication of BP perhaps with more extent than with the GDL. Carbon as material for BP is used mainly as graphite block (electronic grade graphite) or as a carbon–polymer composite, although some other forms have been tested [124].

7.4.1 Synthetic Graphite

Graphite was the first material used as BP, still is the most used at lab scale, mainly because it has an excellent corrosion resistance, high chemical stability and good electrical conductivity.

To produce graphite blocks, a filler is mixed with pitch as binder. Coke is the most used filler although natural graphite, carbon blacks and recycled graphite particles are also used. The coke is usually obtained from petroleum or coal tar pitches. The filler, particularly coke, is first pyrolyzed to release volatiles to avoid the formation of crack or distortions in the final product. Regarding the binder, petroleum and coal tar pitches are commonly used. These pitches are used due to

their high carbon content, ca. 60 % wt, and the fact that they produce a carbon similar to the filler coke after it is carbonized. Other binders used are phenol and epoxy resins. The binder is heated, in order to decrease the viscosity for allowing its mixture with the filler. The filler-pitch mixture, often called carbon paste, is shaped in blocks by extrusion, molding, or cold isostatic pressing (CIP). Controlling the filler particle size and the filler-to-binder ratio will produce the desired material. The carbon blocks are then carbonized at a temperature between 700 °C and 1,000 °C (often called calcination) and graphitized at temperatures above 2,500 °C. The material treated at high temperature is called polycrystalline graphite or synthetic graphite. In order to produce graphite blocks, a two step liquid-phase carbonization is involved, first during the filler coke preparation and then during the carbonization of the binder pitch. The process of forming the graphite block is key to determine the prefered orientation of the filler particles. Extrusion gives flaky or needle like structure along the extrusion direction. By a molding process, the particles are statistically aligned perpendicular to the compression direction. While in CIP, the particles are randomly oriented producing high density isotropic graphite blocks.

The most available graphite plate is made by POCO (Pure Oil Company), a division of Entegris Inc. A variety of high-strength isotropic graphite is produced by POCO where PyroCell is the most known product with very low porosity.

The main drawback of graphite as BP is that flow channels have to be machined on, increasing the cost and the time in mass production. Moreover, a resin impregnation step has to be added post machining of the plate to avoid gas permeation. Such process also increases the cost of the plate. Another problem is the low flexural strength and brittle nature, making the material prone to fracture and forbidding the BPs to be thinner that 5 mm, hence increasing the stack size and weight.

7.4.2 Carbon Composites

Composite is a term that refers to a material prepared by introducing a filler, typically as powder, flakes or fibers, in a continuous matrix in order to obtain a material with better mechanical and corrosion properties. Several composite materials have been assessed as BP material for FC, including carbon–carbon composites, graphite/polymer mixtures (thermoplastic based composites), carbon fiber/epoxy resin (thermosetting based composites), and others conducting fillers with different polymers [8, 125–129]. The most common composites employed are prepared with carbon or graphite filler and a thermoplastic or thermosetting as matrix [130, 131]. The use of the later implies that the plates can be fabricated by injection molding or by hot pressing [126, 131]. The filler is the main responsible for the electrical conductivity of the material, therefore loadings of carbon between 60 % and 90 % by volume are commonly used. However, so high loadings tend to make the plates brittle and therefore suffering similar problems as with synthetic graphite.

The three most common composites used for BP are: carbon/carbon composite (CCC), thermoplastic based composites (TpC) and thermosetting based composites (TsC). The filler in all cases is carbon with a given degree of graphitization. Increasing the graphitization degree increases the electrical conductivity of the composite. However, carbon with low graphitization degree is less expensive, reducing the plate cost. The graphite can be natural or synthetic, the former having a higher graphitization degree but might include some impurities. On the other hand, the synthetic graphite has a higher purity but with a lower degree of graphitization. In all cases the filler is a mixture of graphite and carbon in order to have good conductivity and low cost. The percolation model can give an idea of the maximum conductivity with the lower amount of graphite.

In the CCC the filler is mixed with a resin, commonly phenolic resin, and sintered in a carbonization or graphitization step similar to the fabrication of synthetic graphite. The material obtained has a lower density, typically 20–40 % than synthetic graphite. The CCC allows the use of molding or vacuum molding processes. Lower plate thickness than synthetic graphite can be obtained.

In the TsC the filler is also inserted in a resin matrix, typically phenolic although epoxy and vinyl ester are also used. However, there is not a carbonization step like in the CCC. Due to the similarity in composition, CCC is sometimes confused with TsC. Channel manufacturing in TsC is done by compression molding. Entegris Inc. commercializes TsC BPs based on vinyl ester and phenolic resin.

In the TpC the filler is introduced in a more common plastic such as polypropylene. Even though the use of that kind of plastic reduces the production cost they have a low working temperature (70–80 °C) and mechanical properties that limit the range of applications. Other thermoplastic used as matrix are polyphenylene sulfide (PPS), polyvinylidenefluoride (PVDF), polyarylene disulfide and liquid crystalline polymer (LCP) [130, 132] which might increase the range of applications. TpC allows the use of injection molding process, a very well known industrial process, for channel fabrication. Typical conductivity values reported for TpC materials are 100 S cm^{-1} for the in-plane direction and 20 S cm^{-1} for the through-plane direction [130]. The British company Bac2 produces a TsC composite for BP using a proprietary conducting polymer that cures at room temperature called Electrophen®.

7.5 Conclusions

Carbon compounds are present in almost all the fuel cell components as was described along the chapter.

The catalyst carbon support plays an important role in the catalytic activity and the fuel cell performance. Different carbon supports were reviewed, analyzing their pore size distribution and fuel cell performance. An overview of the fabrication routes used to synthesize them was included. The carbon porosity affects the catalytic activity by modifying the catalyst dispersion, particle size distribution,

alloying degree and mass transport. Several authors concluded that a better FC performance could be achieved when the carbon pore size distribution is above 20 nm improving the contact between the PtRu catalyst, methanol, and perfluorsulfonate ionomer (triple phase boundary) in the anodic layer of a DMFC. These experimental results show that the fabrication of materials with negligible microporosity and mesoporosity larger than 20 nm is a challenge for the synthetic chemist, being very few the materials showing such characteristics. Therefore, the developing of new routes to fabricate carbon with the mentioned tailored structure can be promising for improving the performance of fuel cells fed with methanol. Likewise, these materials could also be considered for other systems that use similar fuels like ethanol or formic acid (liquid fuels), although research with such fuels has just began.

Similarly, research conducted on materials and fabrication methods for GDL and bipolar plates aim to tune their properties in order to improve the fuel cell performance. It is clear that the current trend is the integration of the MEA components in order to improve the architecture of the triple phase boundary region and, consequently, the mass and charge transport.

References

1. Litster S, McLean G (2004) PEM fuel cell electrodes. J Power Sources 130:61–76
2. Mehta V, Cooper JS (2003) Review and analysis of PEM fuel cell design and manufacturing. J Power Sources 114:32–53
3. Zhang J (2008) PEM fuel cell electrocatalysts and catalyst layers: fundamentals and applications. Springer, New York
4. Chen E (2003) Thermodynamics and electrochemical kinetics. In: Hooger G (ed) Fuel cell technology handbook. CRC Press, New York
5. DOE Hydrogen and Fuel Cells Program. 2009 Annual Progress Report (2009) No DOE/GO-102009-2950. U.S. Department of Energy, Washington, DC
6. Marcinkoski J, James BD, Kalinoski JA, Podolski W, Benjamin T, Kopasz J (2011) Manufacturing process assumptions used in fuel cell system cost analyses. J Power Sources 196:5282–5292
7. Baker AA (1975) Carbon fibre reinforced metals – a review of the current technology. Mater Sci Eng 17:177–208
8. Dhakate S, Mathur R, Kakati B, Dhami T (2007) Properties of graphite-composite bipolar plate prepared by compression molding technique for PEM fuel cell. Int J Hydrogen Energy 32:4537–4543
9. Kamarudin SK, Daud WRW, Som AM, Takriff MS, Mohammad AW (2006) Technical design and economic evaluation of a PEM fuel cell system. J Power Sources 157:641–649
10. Bar-On I, Kirchain R, Roth R (2002) Technical cost analysis for PEM fuel cells. J Power Sources 109:71–75
11. Guy R, Lancaster T, Thornton J, Hart A, Sun J, Wilde J (2012) Polymer fuel cells – cost reduction and market potential. Carbon Trust, London
12. Sharma S, Pollet BG (2012) Support materials for PEMFC and DMFC electrocatalysts – a review. J Power Sources 208:96–119

13. Soboleva T, Zhao X, Malek K, Xie Z, Navessin T, Holdcroft S (2010) On the micro-, meso-, and macroporous structures of polymer electrolyte membrane fuel cell catalyst layers. ACS Appl Mater Interfaces 2:375–384
14. Kinoshita K (1988) Carbon: electrochemical and physicochemical properties. Wiley, New Jersey
15. Rodríguez-Reinoso F (1998) The role of carbon materials in heterogeneous catalysis. Carbon 36:159–175
16. Antolini E (2009) Carbon supports for low-temperature fuel cell catalysts. Appl Catal, B 88:1–24
17. Figueiredo JL, Pereira MFR, Freitas MMA, Órfão JJM (2006) Characterization of active sites on carbon catalysts. Ind Eng Chem Res 46:4110–4115
18. Calvillo L, Gangeri M, Perathoner S, Centi G, Moliner R, Lázaro MJ (2011) Synthesis and performance of platinum supported on ordered mesoporous carbons as catalyst for PEM fuel cells: effect of the surface chemistry of the support. Int J Hydrogen Energy 36:9805–9814
19. Uchida M, Aoyama Y, Tanabe M, Yanagihara N, Eda N, Ohta A (1995) Influences of both carbon supports and heat-treatment of supported catalyst on electrochemical oxidation of methanol. J Electrochem Soc 142:2572–2576
20. Liu H, Song C, Zhang L, Zhang J, Wang H, Wilkinson DP (2006) A review of anode catalysis in the direct methanol fuel cell. J Power Sources 155:95–110
21. Takasu Y, Kawaguchi T, Sugimoto W, Murakami Y (2003) Effects of the surface area of carbon support on the characteristics of highly-dispersed PtRu particles as catalysts for methanol oxidation. Electrochim Acta 48:3861–3868
22. Watanabe M, Sei H, Stonehart P (1989) The influence of platinum crystallite size on the electroreduction of oxygen. J Electroanal Chem Interf Electrochem 261:375–387
23. Rao V, Simonov PA, Savinova ER, Plaksin GV, Cherepanova SV, Kryukova GN, Stimming U (2005) The influence of carbon support porosity on the activity of PtRu/Sibunit anode catalysts for methanol oxidation. J Power Sources 145:178–187
24. Aricò AS, Srinivasan S, Antonucci V (2001) DMFCs: from fundamental aspects to technology development. Fuel Cells 1:133–161
25. Uchida M, Fukuoka Y, Sugawara Y, Ohara H, Ohta A (1998) Improved preparation process of very-low-platinum-loading electrodes for polymer electrolyte fuel cells. J Electrochem Soc 145:3708–3713
26. Uchida M, Fukuoka Y, Sugawara Y, Eda N, Ohta A (1996) Effects of microstructure of carbon support in the catalyst layer on the performance of polymer-electrolyte fuel cells. J Electrochem Soc 143:2245–2252
27. Hughes TV, Chambers CR (1889) Manufacture of carbon filaments. US Patent 405,480, 18 June 1889
28. Iijima S (1991) Helical microtubules of graphitic carbon. Nature 354:56–58
29. Serp P, Corrias M, Kalck P (2003) Carbon nanotubes and nanofibers in catalysis. Appl Catal A 253:337–358
30. Drillet J-F, Bueb H, Dittmeyer R, Dettlaff-Weglikowska U, Roth S (2009) Efficient SWCNT-based anode for DMFC applications. J Electrochem Soc 156:F137–F144
31. Jeng K-T, Chien C-C, Hsu N-Y, Yen S-C, Chiou S-D, Lin S-H, Huang W-M (2006) Performance of direct methanol fuel cell using carbon nanotube-supported Pt–Ru anode catalyst with controlled composition. J Power Sources 160:97–104
32. Prabhuram J, Zhao TS, Tang ZK, Chen R, Liang ZX (2006) Multiwalled carbon nanotube supported PtRu for the anode of direct methanol fuel cells. J Phys Chem B 110:5245–5252
33. Tsuji M, Kubokawa M, Yano R, Miyamae N, Tsuji T, Jun M-S, Hong S, Lim S, Yoon S-H, Mochida I (2006) Fast preparation of PtRu catalysts supported on carbon nanofibers by the microwave-polyol method and their application to fuel cells. Langmuir 23:387–390
34. Joo SH, Pak C, You DJ, Lee S-A, Lee HI, Kim JM, Chang H, Seung D (2006) Ordered mesoporous carbons (OMC) as supports of electrocatalysts for direct methanol fuel cells

(DMFC): effect of carbon precursors of OMC on DMFC performances. Electrochim Acta 52:1618–1626
35. Chang H, Joo SH, Pak C (2007) Synthesis and characterization of mesoporous carbon for fuel cell applications. J Mater Chem 17:3078–3088
36. Pekala RW (1989) Low density, resorcinol-formaldehyde aerogels. US Patent 4,873,218, 10 Oct 1989
37. Yamamoto T, Mukai SR, Endo A, Nakaiwa M, Tamon H (2003) Interpretation of structure formation during the sol-gel transition of a resorcinol-formaldehyde solution by population balance. J Colloid Interf Sci 264:532–537
38. Aegerter MA, Leventis N, Koebel MM (2011) Aerogels handbook. Springer, New York
39. Job N, Théry A, Pirard R, Marien J, Kocon L, Rouzaud J-N, Béguin F, Pirard J-P (2005) Carbon aerogels, cryogels and xerogels: influence of the drying method on the textural properties of porous carbon materials. Carbon 43:2481–2494
40. Takashi K (2000) Control of pore structure in carbon. Carbon 38:269–286
41. Lu AH, Spliethoff B, Schüth F (2008) Aqueous synthesis of ordered mesoporous carbon via self-assembly catalyzed by amino acid. Chem Mater 20:5314–5319
42. Zhang F, Meng Y, Gu D, Yan Y, Yu C, Tu B, Zhao D (2005) A facile aqueous route to synthesize highly ordered mesoporous polymers and carbon frameworks with Ia3d bicontinuous cubic structure. J Am Chem Soc 127:13508–13509
43. Al-Muhtaseb SA, Ritter JA (2003) Preparation and properties of resorcinol–formaldehyde organic and carbon gels. Adv Mater 15:101–114
44. Du H, Li B, Kang F, Fu R, Zeng Y (2007) Carbon aerogel supported Pt–Ru catalysts for using as the anode of direct methanol fuel cells. Carbon 45:429–435
45. Calderón JC, Mahata N, Pereira MFR, Figueiredo JL, Fernandes VR, Rangel CM, Calvillo L, Lázaro MJ, Pastor E (2012) Pt-Ru catalysts supported on carbon xerogels for PEM fuel cells. Int J Hydrogen Energy 37:7200–7211
46. Mahata N, Silva AR, Pereira MFR, Freire C, de Castro B, Figueiredo JL (2007) Anchoring of a [Mn(salen)Cl] complex onto mesoporous carbon xerogels. J Colloid Interf Sci 311:152–158
47. Arbizzani C, Beninati S, Soavi F, Varzi A, Mastragostino M (2008) Supported PtRu on mesoporous carbons for direct methanol fuel cells. J Power Sources 185:615–620
48. Knox JH, Kaur B, Millward GR (1986) Structure and performance of porous graphitic carbon in liquid chromatography. J Chromatogr A 352:3–25
49. Ryoo R, Joo SH, Jun S (1999) Synthesis of highly ordered carbon molecular sieves via template-mediated structural transformation. J Phys Chem B 103:7743–7746
50. Vinu A, Mori T, Ariga K (2006) New families of mesoporous materials. Sci and Technol Adv Mat 7:753–771
51. Lee KT, Oh SM (2002) Novel synthesis of porous carbons with tunable pore size by surfactant-templated sol-gel process and carbonisation. Chem Commun 22:2722–2723
52. Lu AH, Schüth F (2006) Nanocasting: a versatile strategy for creating nanostructured porous materials. Adv Mater 18:1793–1805
53. Ryoo R, Joo SH, Jun S, Tsubakiyama T, Terasaki O (2001) Ordered mesoporous carbon molecular, sieves by templated synthesis: the structural varieties. In: Galarneau A, Fajula F, Renzo FD, Vedrine J (eds) Studies in surface science and catalysis. Elsevier, Amsterdam
54. Shin HJ, Ryoo R, Kruk M, Jaroniec M (2001) Modification of SBA-15 pore connectivity by high-temperature calcination investigated by carbon inverse replication. Chem Commun 4:349–350
55. Liu X, Tian B, Yu C, Gao F, Xie S, Tu B, Che R, Peng L-M, Zhao D (2002) Room-temperature synthesis in acidic media of large-pore three-dimensional bicontinuous mesoporous silica with Ia3d symmetry. Angew Chem Int Ed 41:3876–3878
56. Lu AH, Schmidt W, Spliethoff B, Schüth F (2003) Synthesis of ordered mesoporous carbon with bimodal pore system and high pore volume. Adv Mater 15:1602–1606
57. Fuertes AB (2003) Template synthesis of mesoporous carbons with a controlled particle size. J Mater Chem 13:3085–3088

58. Lu AH, Zhao D, Wan Y (2009) Nanocasting: a versatile strategy for creating nanostructured porous materials. Royal Society of Chemistry, London
59. Stein A, Wang Z, Fierke MA (2009) Functionalization of porous carbon materials with designed pore architecture. Adv Mater 21:265–293
60. Jun S, Joo SH, Ryoo R, Kruk M, Jaroniec M, Liu Z, Ohsuna T, Terasaki O (2000) Synthesis of new, nanoporous carbon with hexagonally ordered mesostructure. J Am Chem Soc 122:10712–10713
61. Chai GS, Yoon SB, Yu J-S, Choi J-H, Sung Y-E (2004) Ordered porous carbons with tunable pore sizes as catalyst supports in direct methanol fuel cell. J Phys Chem B 108:7074–7079
62. Qi J, Jiang L, Tang Q, Zhu S, Wang S, Yi B, Sun G (2012) Synthesis of graphitic mesoporous carbons with different surface areas and their use in direct methanol fuel cells. Carbon 50:2824–2831
63. Ding J, Chan K-Y, Ren J, F-s X (2005) Platinum and platinum–ruthenium nanoparticles supported on ordered mesoporous carbon and their electrocatalytic performance for fuel cell reactions. Electrochim Acta 50:3131–3141
64. Kim P, Kim H, Joo JB, Kim W, Song IK, Yi J (2005) Preparation and application of nanoporous carbon templated by silica particle for use as a catalyst support for direct methanol fuel cell. J Power Sources 145:139–146
65. Zhao D (2012) Ordered mesoporous materials. Wiley, New Jersey
66. Liang C, Dai S (2006) Synthesis of mesoporous carbon materials via enhanced hydrogen-bonding interaction. J Am Chem Soc 128:5316–5317
67. Bell W, Dietz S (2001) Mesoporous carbons and polymers. US Patent 6,297,293, 2 Oct 2001
68. Fujikawa D, Uota M, Sakai G, Kijima T (2007) Shape-controlled synthesis of nanocarbons from resorcinol–formaldehyde nanopolymers using surfactant-templated vesicular assemblies. Carbon 45:1289–1295
69. Fujikawa D, Uota M, Yoshimura T, Sakai G, Kijima T (2006) Surfactant-templated synthesis of resorcinol-formaldehyde polymer and carbon nanostructures: nanospheres and nanowires. Chem Lett 35:432–433
70. Nishiyama N, Zheng T, Yamane Y, Egashira Y, Ueyama K (2005) Microporous carbons prepared from cationic surfactant–resorcinol/formaldehyde composites. Carbon 43:269–274
71. Bruno MM, Cotella NG, Miras MC, Barbero CA (2010) A novel way to maintain resorcinol—formaldehyde porosity during drying: stabilization of the sol–gel nanostructure using a cationic polyelectrolyte. Colloids Surface A 362:28–32
72. Liang C, Hong K, Guiochon GA, Mays JW, Dai S (2004) Synthesis of a large-scale highly ordered porous carbon film by self-assembly of block copolymers. Angew Chem Int Ed 43:5785–5789
73. Pantea D, Darmstadt H, Kaliaguine S, Sümmchen L, Roy C (2001) Electrical conductivity of thermal carbon blacks: influence of surface chemistry. Carbon 39:1147–1158
74. Tanaka S, Nishiyama N, Egashira Y, Ueyama K (2005) Synthesis of ordered mesoporous carbons with channel structure from an organic-organic nanocomposite. Chem Commun 16:2125–2127
75. Xu J, Wang A, Zhang T (2012) A two-step synthesis of ordered mesoporous resorcinol–formaldehyde polymer and carbon. Carbon 50:1807–1816
76. Wang X, Liang C, Dai S (2008) Facile synthesis of ordered mesoporous carbons with high thermal stability by self-assembly of resorcinol − formaldehyde and block copolymers under highly acidic conditions. Langmuir 24:7500–7505
77. Meng Y, Gu D, Zhang F, Shi Y, Yang H, Li Z, Yu C, Tu B, Zhao D (2005) Ordered mesoporous polymers and homologous carbon frameworks: amphiphilic surfactant templating and direct transformation. Angew Chem Int Ed 44:7053–7059
78. Meng Y, Gu D, Zhang F, Shi Y, Cheng L, Feng D, Wu Z, Chen Z, Wan Y, Stein A, Zhao D (2006) A family of highly ordered mesoporous polymer resin and carbon structures from organic − organic self-assembly. Chem Mater 18:4447–4464

79. Deng Y, Yu T, Wan Y, Shi Y, Meng Y, Gu D, Zhang L, Huang Y, Liu C, Wu X, Zhao D (2007) Ordered mesoporous silicas and carbons with large accessible pores templated from amphiphilic diblock copolymer poly(ethylene oxide)-b-polystyrene. J Am Chem Soc 129:1690–1697
80. Atiyeh H, Karan K, Peppley B, Phoenix A, Halliop E, Pharoah J (2007) Experimental investigation of the role of a microporous layer on the water transport and performance of a PEM fuel cell. J Power Sources 170:111–121
81. Thomas YRJ, Bruno MM, Corti HR (2012) Characterization of a monolithic mesoporous carbon as diffusion layer for micro fuel cells application. Micropor Mesopor Mat 155:47–55
82. Krishnamurthy B, Deepalochani S (2009) Effect of PTFE content on the performance of a Direct Methanol fuel cell. Int J Hydrogen Energy 34:446–452
83. Wilkinson DP, Zhang J, Hui R, Fergus J, Li X (2009) Proton exchange membrane fuel cells: materials, properties and performance. CRC Press, London
84. Akio S (1964) On the carbonization of polyacrylonitrile fiber. Carbon 1:391–392
85. Shindo A, Fujii R, Sengoku T (1959) Method for manufacturing carbon product from acrylonitrile synthetic macromolecular substance. Japan Patent 37–4405
86. Greiner A, Wendorff JH (2007) Electrospinning: a fascinating method for the preparation of ultrathin fibers. Angew Chem Int Ed 46:5670–5703
87. Sutasinpromprae J, Jitjaicham S, Nithitanakul M, Meechaisue C, Supaphol P (2006) Preparation and characterization of ultrafine electrospun polyacrylonitrile fibers and their subsequent pyrolysis to carbon fibers. Polym Int 55:825–833
88. Mittal J, Mathur RB, Bahl OP (1997) Post spinning modification of PAN fibres – a review. Carbon 35:1713–1721
89. Yusof N, Ismail AF (2012) Post spinning and pyrolysis processes of polyacrylonitrile (PAN)-based carbon fiber and activated carbon fiber: a review. J Anal Appl Pyrol 93:1–13
90. Pierson HO (1995) Handbook of carbon, graphite, diamonds and fullerenes: processing, properties and applications. Noyes Publications, New Jersey
91. Ko T-H, Chiranairadul P, Lin C-H (1991) The influence of continuous stabilization on the properties of stabilized fibers and the final activated carbon fibers. Part I. Polym Eng Sci 31:1618–1626
92. Donnet JB (1998) Carbon fibers. CRC Press, New York
93. Zhang X, Shen Z (2002) Carbon fiber paper for fuel cell electrode. Fuel 81:2199–2201
94. Mathur RB, Maheshwari PH, Dhami TL, Tandon RP (2007) Characteristics of the carbon paper heat-treated to different temperatures and its influence on the performance of PEM fuel cell. Electrochim Acta 52:4809–4817
95. Liu C-H, Ko T-H, Liao Y-K (2008) Effect of carbon black concentration in carbon fiber paper on the performance of low-temperature proton exchange membrane fuel cells. J Power Sources 178:80–85
96. Mathur RB, Maheshwari PH, Dhami TL, Sharma RK, Sharma CP (2006) Processing of carbon composite paper as electrode for fuel cell. J Power Sources 161:790–798
97. Toray carbon paper specification (2005) http://www.torayca.com/en/index.html. Accessed 18 July 2012
98. Ballard gas difussion layer (2012) http://www.ballard.com/material-products/gas-diffusion.aspx. Accessed 18 July 2012
99. Liu C-H, Ko T-H, Kuo W-S, Chou H-K, Chang H-W, Liao Y-K (2009) Effect of carbon fiber cloth with different structure on the performance of low temperature proton exchange membrane fuel cells. J Power Sources 186:450–454
100. Ko T-H, Liao Y-K, Liu C-H (2007) Effects of graphitization of PAN-based carbon fiber cloth on its use as gas diffusion layers in proton exchange membrane fuel cells. New Carbon Mater 22:97–101
101. Wei J, Liang P, Huang X (2011) Recent progress in electrodes for microbial fuel cells. Bioresource Technol 102:9335–9344
102. Dicks AL (2006) The role of carbon in fuel cells. J Power Sources 156:128–141

103. Qi Z, Kaufman A (2002) Improvement of water management by a microporous sublayer for PEM fuel cells. J Power Sources 109:1–9
104. Tucker MC, Odgaard M, Lund PB, Yde-Andersen S, Thomas JO (2005) The pore structure of direct methanol fuel cell electrodes. J Electrochem Soc 152:A1844–A1844
105. Park G-G, Sohn Y-J, Yang T-H, Yoon Y-G, Lee W-Y, Kim C-S (2004) Effect of PTFE contents in the gas diffusion media on the performance of PEMFC. J Power Sources 131:182–187
106. Velayutham G (2011) Effect of micro-layer PTFE on the performance of PEM fuel cell electrodes. Int J Hydrogen Energy 36:14845–14850
107. Sun X, Saha MS (2008) Nanotubes, nanofibers and nanowires as supports for catalysts. In: Zhang J (ed) PEM fuel cell electrocatalysts and catalyst layers: fundamentals and applications. Springer, New York
108. Lin G, Nguyen TV (2005) Effect of thickness and hydrophobic polymer content of the gas diffusion layer on electrode flooding level in a PEMFC. J Electrochem Soc 152: A1942–A1948
109. Oedegaard A, Hebling C, Schmitz A, Møller-Holst S, Tunold R (2004) Influence of diffusion layer properties on low temperature DMFC. J Power Sources 127:187–196
110. Wang X, Zhang H, Zhang J, Xu H, Tian Z, Chen J, Zhong H, Liang Y, Yi B (2006) Microporous layer with composite carbon black for PEM fuel cells. Electrochim Acta 51:4909–4915
111. Wang T, Lin C, Fang Y, Ye F, Miao R, Wang X (2008) A study on the dissymmetrical microporous layer structure of a direct methanol fuel cell. Electrochim Acta 54:781–785
112. Chen-Yang YW, Hung TF, Huang J, Yang FL (2007) Novel single-layer gas diffusion layer based on PTFE/carbon black composite for proton exchange membrane fuel cell. J Power Sources 173:183–188
113. Du H-Y, Wang C-H, Hsu H-C, Chang S-T, Yen S-C, Chen L-C, Viswanathan B, Chen K-H (2011) High performance of catalysts supported by directly grown PTFE-free micro-porous CNT layer in a proton exchange membrane fuel cell. J Mater Chem 21:2512–2516
114. Tang Z, Poh CK, Tian Z, Lin J, Ng HY, Chua DHC (2011) In situ grown carbon nanotubes on carbon paper as integrated gas diffusion and catalyst layer for proton exchange membrane fuel cells. Electrochim Acta 56:4327–4334
115. Jeng K-T, Chien C-C, Hsu N-Y, Huang W-M, Chiou S-D, Lin S-H (2007) Fabrication and impedance studies of DMFC anode incorporated with CNT-supported high-metal-content electrocatalyst. J Power Sources 164:33–41
116. Wang CH, Du HY, Tsai YT, Chen CP, Huang CJ, Chen LC, Chen KH, Shih HC (2007) High performance of low electrocatalysts loading on CNT directly grown on carbon cloth for DMFC. J Power Sources 171:55–62
117. Gao Y, Sun GQ, Wang SL, Zhu S (2010) Carbon nanotubes based gas diffusion layers in direct methanol fuel cells. Energy 35:1455–1459
118. Gerteisen D, Heilmann T, Ziegler C (2008) Enhancing liquid water transport by laser perforation of a GDL in a PEM fuel cell. J Power Sources 177:348–354
119. Gerteisen D, Sadeler C (2010) Stability and performance improvement of a polymer electrolyte membrane fuel cell stack by laser perforation of gas diffusion layers. J Power Sources 195:5252–5257
120. Manahan MP, Hatzell MC, Kumbur EC, Mench MM (2011) Laser perforated fuel cell diffusion media. Part I: Related changes in performance and water content. J Power Sources 196:5573–5582
121. Bruno MM, Corti HR, Balach J, Cotella NG, Barbero CA (2009) Hierarchical porous materials: capillaries in nanoporous carbon. Funct Mat Lett 2:135–138
122. Bruno MM, Franceschini EA, Viva FA, Thomas YRJ, Corti HR (2012) Electrodeposited mesoporous platinum catalysts over hierarchical carbon monolithic support as anode in small PEM fuel cells. Int J Hydrogen Energy 37:14911–14919

123. DOE Hydrogen and Fuel Cells Program. 2011 Annual Progress Report (2011) No DOE/GO-102011-3422. U.S. Department of Energy, Washington, DC
124. Middelman E, Kout W, Vogelaar B, Lenssen J, de Waal E (2003) Bipolar plates for PEM fuel cells. J Power Sources 118:44–46
125. Blunk R, Abd Elhamid MH, Lisi D, Mikhail Y (2006) Polymeric composite bipolar plates for vehicle applications. J Power Sources 156:151–157
126. Heinzel A, Mahlendorf F, Niemzig O, Kreuz C (2004) Injection moulded low cost bipolar plates for PEM fuel cells. J Power Sources 131:35–40
127. Kim M, Yu HN, Lim JW, Lee DG (2012) Bipolar plates made of plain weave carbon/epoxy composite for proton exchange membrane fuel cell. Int J Hydrogen Energy 37:4300–4308
128. Lee Y-B, Lee C-H, Kim K-M, Lim D-S (2011) Preparation and properties on the graphite/polypropylene composite bipolar plates with a 304 stainless steel by compression molding for PEM fuel cell. Int J Hydrogen Energy 36:7621–7627
129. Mathur RB, Dhakate SR, Gupta DK, Dhami TL, Aggarwal RK (2008) Effect of different carbon fillers on the properties of graphite composite bipolar plate. J Mater Process Tech 203:184–192
130. Huang J, Baird DG, McGrath JE (2005) Development of fuel cell bipolar plates from graphite filled wet-lay thermoplastic composite materials. J Power Sources 150:110–119
131. Chen W, Liu Y, Xin Q (2010) Evaluation of a compression molded composite bipolar plate for direct methanol fuel cell. Int J Hydrogen Energy 35:3783–3788
132. de Oliveira MCL, Ett G, Antunes RA (2012) Materials selection for bipolar plates for polymer electrolyte membrane fuel cells using the Ashby approach. J Power Sources 206:3–13

View publication stats